

Large scale Binder jet printing using waste materials

Master in Product Design Engineering

João Afonso Lupi de Ordaz Caldeira

Leiria, December of 2020



Large scale Binder jet printing using waste materials

Master in Product Design Engineering

João Afonso Lupi de Ordaz Caldeira

Master's Project held under the guidance of Doctor Fábio Simões, Professor of the Higher School of Technology and Management of the Polytechnic Institute of Leiria and co-orientation of Doctor (s) Artur Mateus, Professor at the Higher School of Technology and Management of the Polytechnic Institute of Leiria.

Leiria, December of 2020.

Originality and Copyright

This dissertation/project report is original, made only for this purpose, and all authors whose studies and publications were used to complete it are duly acknowledged. Partial reproduction of this document is authorized, provided that the Author is explicitly mentioned, as well as the study cycle, i.e., Master in Product Design Engineering, 2019/2020 academic year, of the School of Technology and Management of the Polytechnic Institute of Leiria, and the date of the public presentation of this work.

Dedication

For the help and company this last year, for all the easiness gained to concentrate on this project without major distractions caused by everyday life and the readiness of giving. I dedicate this project to my girlfriend Margarida.

Acknowledgements

I want to acknowledge who played a role in the project accomplishment. First of all, my parents, who support me with love, understanding and knowledge. My girlfriend, who helped me every step of the way without hesitation.

Secondary, my committee members, each of whom has provided patient advice and guidance throughout the research process. Moreover, my college Rafael for facilitating stays while researching at Leiria. Thank you all for your unwavering support.

Abstract

Additive manufacturing (AM) is especially suited for unique objects or low production batches since it does not require expensive tooling. The AM market has undergone enormous growth, even though there is still a significant limitation in this technology type when producing large parts.

Powder bed technology, particularly binder jetting, allows the production of several types of materials. The print size is directly related to the machine's build volume size when using powder bed technology. Moreover, materials used in powder bed processes are usually high-cost materials, making large prints not affordable. Instead of working with high-cost types of powder, it is possible to replace them with low cost, biodegradable materials, like wood, or waste materials like ground tire (GTW). Using materials such as this allows low-cost production parts while contributing to the incorporation of residues that otherwise would have to be discarded, with a low environmental impact.

This work studies the usage of waste materials in small grains and calibrated dust with different sizes as a matrix in a binder jetting machine with a build volume of 1 m^3 . Wood dust and GTW are being studied and additives can be added to the bulk material to affect the powder deposit ability, printing behavior, final part properties and post-processing behavior.

It was possible to produce test specimens, but the machine had to be refilled each layer manually. The rest of the printing process was made automatically, producing specimens that were tested successfully.

Keywords: Additive manufacturing, Binder jetting, Ground tire rubber, Polyvinyl Alcohol, Sustainability, Wood

Resumo

A maquinação aditiva é especialmente adequada para objetos exclusivos ou lotes de baixa produção, uma vez que não requer ferramentas caras. O mercado de maquinação aditiva passou por um enorme crescimento, embora ainda exista uma limitação significativa desse tipo de tecnologia na produção de peças grandes.

A tecnologia de powder bed, principalmente binder jetting, permite a produção de diversos tipos de materiais. O tamanho da impressão está diretamente relacionado ao tamanho do volume de construção da máquina ao usar a tecnologia de powder bed. Além disso, os materiais usados em processos de powder bed são geralmente materiais de alto custo, tornando as impressões grandes não acessíveis. Em vez de trabalhar com tipos de pó de alto custo, é possível substituí-los por materiais biodegradáveis de baixo custo, como madeira, ou resíduos como pneu moído. A utilização de materiais como este permite a produção de peças de baixo custo, ao mesmo tempo que contribui para a incorporação de resíduos que, de outra forma, teriam que ser descartados, com baixo impacto ambiental.

Este trabalho estuda o uso de materiais residuais em pequenos grãos e pó calibrado com diferentes tamanhos como matriz numa máquina de binder jetting com volume de construção de $1m^3$. Pó de madeira e pneu moído estão a ser estudados e aditivos podem ser adicionados ao material a granel para afetar a capacidade de depósito de pó, comportamento de impressão, propriedades da peça final e comportamento de pós-processamento.

Foi possível produzir provetes de teste, mas a máquina teve que ser recarregada a cada camada manualmente. O resto do processo de impressão foi feito automaticamente, produzindo amostras que foram testadas com sucesso.

Palavras-chave: *(Maquinação aditiva, Binder jetting, Pneu moído, Álcool polivinílico, Sustentabilidade, Madeira)*

List of Figures

2.1	AM concrete wall [2]	5
2.2	XtreeE System [3]	5
2.3	ProJet CJP 860Pro. Construction volume: 508 x 381 x 229 mm [5]	5
2.4	S-MAX Pro. Construction volume: 1800 x 1000 x 700 mm [1]	6
2.5	compressive strength a) Acrodur coated (red top); uncoated (green center); Lupamin coated (blue bottom) b) stearin (green top)	7
2.6	Counter-rotating roller	9
3.1	Scheme for binder tests	13
3.2	Aquaseal temperature tests	14
3.3	Polyvinyl Alcohol temperature tests	15
3.4	Acrodur 950L temperature tests	16
3.5	Acrodur drop. As it can be observed, the binder material did no impregnated the dust.	16
3.6	Test pieces silicon molds. The moulds contain 100 μm of wood, 100 μm to 400 μm of waste tire powders (WTP) and 400 μm of wood (respectively) with a 30% aquaseal binder ratio.	17
3.7	Results (from left to right) 100 μm - 400 μm WTP, 400 μm wood, 500 μm - 800 μm waste tire powders (WTP) and 100 μm wood with 30% binder ratio.	18
3.8	Results (from left to right) 100 μm wood, 100 μm - 400 μm WTP, 500 μm - 800 μm WTP and 400 μm wood with 50% binder ratio. WTP- waste tire powders	18

3.9	Results (from left to right) 100 μm - 400 μm WTP, 500 μm - 800 μm WTP, 100 μm wood and 400 μm wood with 70% binder ratio. WTP- waste tire powders	18
3.10	Testing platform. Source: CDRSP - Center to Rapid and Sustainable Product Development, Polytechnic Institute of Leiria, Portugal	19
3.11	Testing platform. Source: CDRSP - Center to Rapid and Sustainable Product Development, Polytechnic Institute of Leiria, Portugal	19
3.12	Mask to delimit binder drop area.	20
3.13	Cylindrical elevation system. The green parts are the build base and the extreme walls of the construction build, the blue components are the mechanical parts that create the vertical movement. Source: CDRSP - Center to Rapid and Sustainable Product Development, Polytechnic Institute of Leiria, Portugal	21
3.14	Aquaseal drops on a layer of 200 μm particle size wood dust.	24
4.1	Counter-rotating roller parts.	26
4.2	Dust trimmer box made out of coriboard.	27
4.3	Peristaltic pump	27
4.4	1 mm nozzle.	28
4.5	Support to hold the peristaltic pump.	28
4.6	Two litter binder deposit.	29
4.7	Deposit support attached to printer arm.	29
4.8	Hose adapter.	30
4.9	Hose brake.	30
4.10	Deposit cover.	30
4.11	Nozzle stabilizer and the bolts and nuts to assemble it to the nozzle.	31
4.12	PVA line on the wood dust layer injected with a peristaltic pump through a 1 mm nozzle.	31

4.13 6,15 mm diameter nozzle.	32
4.14 Polyvinyl alcohol line on the wood dust layer injected with a peristaltic pump through a 6,15 mm nozzle.	32
4.15 Image on the left: - Direct acting solenoid valve components. Image on the right: - SLA 3D printed solenoid valve with white resin.	33
4.16 Valve connector. SLA printed part to connect the deposit tube to the solenoid valve system.	34
4.17 Bender deposition speed test.	35
4.18 EdingCNC program interface.	36
4.19 Binder deposition.	37
4.20 Spiral path.	38
4.21 Zigzag path.	38
5.1 Printing machine with the components created for the project.	41
5.2 Test specimen measures according to the ASTM D638 standard.	41
5.3 Test sample bottom.	42
5.4 Spiral tests printing overview.	43
5.5 Binder path (gray line) versus nozzle path (dashed line).	43
5.6 Test 11 stress-strain curve.	44
5.7 Spiral method printed batch.	45

List of Tables

3.1	Wood and waste tire powders (WTP) materials weight mixture with 30% Aquaseal ratio.	17
3.2	Wood and waste tire powders (WTP) materials weight mixture with 50% Aquaseal ratio.	17
3.3	Wood and waste tire powders (WTP) materials weight mixture with 70% Aquaseal ratio.	17
3.4	Ground tire waste (GTR) coated with polyvinyl alcohol (PVA) test samples tensile properties table	22
3.5	Dust wood soaked with polyvinyl alcohol (PVA) test samples tensile properties table	22
3.6	Dust Wood soaked with polyvinyl alcohol (PVA) and cyanocrylate test samples tensile properties table	23
3.7	Ground Tire Waste (GTR) soaked with polyvinyl alcohol (PVA) and cyanocrylate test samples tensile properties table	23
5.1	Specimens tests performed using the spiral method and soaked with cyanoacrylate. This tests refer to the yield strength (σ_y) in megapascal (MPa), the Ultimate tensile strength (UTS) in megapascal (MPa), the nominal strain (ϵ) and Young's modulus (E) in megapascal (MPa).	45
5.2	Specimens tests performed using the zigzag method and soaked with cyanoacrylate. This tests refer to the yield strength (σ_y) in megapascal (MPa), the Ultimate tensile strength (UTS) in megapascal (MPa), the nominal strain (ϵ) and Young's modulus (E) in megapascal (MPa)	46

List of symbols

AM	Additive Manufacturing
BJ	Binder Jet
°C	Celsius degrees
CDRSP	Centro para o Desenvolvimento Rápido e Sustentavel do Produto
DP	Direct Printing
ESTG	Escola Superior de Tecnologia e Gestão
FDM	Fuse Deposit Modeling
GTW	Ground Tire Waste
GTR	Ground Tire Rubber
IB	Inner Bond
MF	Melamine-Formaldehyde
L	Length
mm	Millimeters
MPa	Megapascal
PF	Phenol formaldehyde resins
PFPBNDT	Plastic Fluid Precision Blunt Needle Dispense Tip
PVA	Polyvinyl Alcohol
PSD	Percentual Standard Deviation
UF	Urea-formaldehyde resin
RT	Room temperature
SLA	Stereolithography
SLS	Selective Laser Sintering
WTP	Waste tire Powder
WRC	Wood-Rubber Composite
%	Percentage

Contents

Originality and Copyright	III
Acknowledgements	V
Abstract	VII
Resumo	IX
List of Figures	XIII
List of Tables	XV
List of symbols	XVII
1 Introduction	1
1.1 Theoretical Framework	1
1.2 Research Objectives	2
1.3 General structure	2
2 Literature review	4
2.1 Binder Jet	4
2.2 Binder Jet using natural materials	6
2.3 Binder Jet with powder mixtures	7
2.4 Process development	8
2.4.1 Formulation of the powder	8
2.4.2 Selection of a binding method	9
2.4.3 Formulation of the liquid binder	10
2.5 Literature Review Conclusions	11
3 Experimental Materials and Procedures	12
3.1 Test plans	12
3.2 Materials and equipment	12
3.3 Binder drop	13
3.3.1 Aquaseal	14
3.3.2 PVA	15
3.3.3 Acrodur 950L	15
3.4 Binder coating	16
3.5 Layer Experiments	18
3.5.1 Testing Platform	20
3.5.2 Polyvinyl alcohol Tests	20
3.5.3 Aquaseal Tests	23
4 Equipment	25
4.1 Counter-rotating roller	25
4.2 Dust trimmer	25
4.3 Binder deposition	26

4.3.1	Peristaltic pump	26
4.3.2	Solenoid valve	33
4.3.3	Deposition parameters	35
4.4	CNC software parameters	35
4.4.1	Creation of the Gcode	36
4.4.2	Material addition	36
4.4.3	Layer creation	37
4.4.4	Binder deposition	37
4.4.5	Ground tire rubber testing	37
5	Results	40
5.1	Print results	42
5.2	Cyanoacrylate absorption	42
5.3	Tensile tests	43
5.3.1	Spiral method	44
5.3.2	Zigzag method	46
5.4	Discussion	46
5.4.1	Prediction Model	47
6	Conclusions	49
	Bibliography	51

1 Introduction

1.1 Theoretical Framework

Additive manufacturing (AM) machines use recent technologies to create objects that do not require expensive and time-consuming handcraft or industrial molding machines. So, supposing a short production series for a specific project or a need for a physical mock-up before mass-producing an object, AM is now one solution that the industry has. As flexible as this technology can be, it still has some constraints. An important one is a limited size, especially in powder bed technology. Despite that, AM technologies market has undergone enormous growth with increasing, there is still a significant limitation in this type of technology when producing large parts.

When using powder bed AM technology, the print size is directly related to the machine's build volume size. When the build volume has to be bigger, the machine has to grow as well. Also, the materials used in powder bed machines are usually high-cost materials making large prints not affordable. Powder bed technology, particularly binder jetting, works to allow the process of several different types of materials. So instead of working with high-cost and nonbiodegradable types of dust, it is possible to replace them with biodegradable materials, like wood, or with reusable materials like ground tire waste (GTW). Using materials such as this allows the creation of low-cost parts with a low environmental impact.

Using AM to manufacture in large-scale objects can be found in the housing construction industry; research uses AM to automate concrete walls' construction. These machines use a similar technology to fuse deposit modeling (FDM) to extrude concrete.

On the other hand, binder jetting (BJ), an AM process, has, so far, the capacity to print the maximum size of 1800 x 1000 x 700 mm build volume using the machine S-MAX Pro [1].

With BJ technology, it is possible to combine dye additives to obtain parts with different colors or luminescent properties. Thus it is also possible to change its appearance through temperature or incident light. It can also include liquid crystals to obtain a transparent part, according to incident light or temperature. It is also possible to add fibers in the pieces' production, strengthening their structure, or creating 4D materials with dynamic elements that change their shape according to the parts incident temperature.

1.2 Research Objectives

The main reason for this project is to reuse waste materials in applications with an extended lifetime. This project aims to contribute to resolving this problem by developing an optimized additive manufacturing technology to construct large scale parts, offering a modular solution with different systems. These systems rely on the deposition of a binder solution on the material bed, which may be granulated, powder, or other—developing a large-scale AM process based on the Binder-Jetting principle, using waste products as the base material.

The project undergoing this study has only the reuse of waste materials necessity. The biodegradability is secondary due to its primary purpose: manufacture urban furniture, which means that the printed part needs to be resistant and endure time before being disposed of or reused.

This project will study the application of two materials, wood and used tire, as filler materials in a binding additive manufacturing process. It proposes a response to a market need when producing large-scale parts of small and medium-sized series, without forgetting the sustainability factor, using materials resulting from industrial waste or similar ones—proposing, as a subject, the production of urban furniture products.

It will be studied scraped wood and ground tire rubber (GTR) calibrated dust with different sizes. These materials will be spread into layers to test the different types of binders and binder spread techniques.

1.3 General structure

The presented study is divided into several chapters. The initial part presents the framework to the project, constituted by a bibliographic review of the concepts used, the materials applied in the study object's development, and an allusion to the experimental methods used.

The data obtained by the experiments and tests carried out will be discussed later, with detailed tables and graphs being exposed, which support the steps ahead of the study.

The work presented consists of 6 parts, starting with the formalities for presenting the report, including a summary, list of tables, figures and acronyms.

This chapter, called “Introduction”, sets out the objectives and motivations that drove the project to this task. The introduction is then followed by the chapter, where the state of the art is exposed.

The third part portrays the materials and the experimental processes used, showing the base material's characteristics, its processing and the tests to which it was submitted. It is especially focused on finding an appropriate binder for the project.

The fourth chapter shows the steps the project took to develop the physical machine and program the gcode to print test specimens. As a physical machine, it is meant to describe; an assembled component to spread layers (counter-rotating roller), another to catch and reuse leftover material, and keep the machine's area around clean (dust trimmer), a component to hold the binder material (deposit) and another to spread it (nozzle system).

The fifth chapter is where the experimental work values are shown, and the results' discussion is also presented.

The sixth module presents conclusions and future work. In the course of the process, new windows for seeking answers have been opened, which for lack of time and for being beyond the initial objectives, will have to be left for other opportunities.

2 Literature review

Large scale 3D Printing frequently aims to automate the housing construction industry. The most common material used for this kind of project is concrete. The material is extruded through a nozzle using a similar concept of FDM technology, as seen in figure 2.2. This technology has stability and precision problems. Contrary to this additive manufacturing technology, traditional methods can create steel rods that fortify the concrete wall structure. Also, as seen in figure 2.1, the wall is left with thick layers that make problems in the final product precision.

The printing method classification described in this report is Powder Bed 3D Printing, particularly BJ. This method facilitates the re-utilization of various materials, like, materials that stop serving their purpose because of their small size. BJ technology is also able to maintain good precision and smooth finish that depends on the particle size. The possibility of reusing materials is the main reason for choosing this technology.

2.1 Binder Jet

BJ is a process that uses two materials, a powder-based material, used to form layers and absorb the binder, and the usually liquid binder itself. The binder fills the powder particles' spaces and binds the layers; it makes the final craft object solid and resistant. A print head moves along the horizontal axes depositing the binder while drawing the layers. Once the counter-rotating roller creates the layer, the build platform lowers, allowing the beginning of another layer process [4]. 3D Printers use this technology, with a larger than usual net build volumes, available on the market as the ProJet CJP 860Pro (figure2.3) and S-MAX Pro (figure 2.4).

BJ can achieve a high precision final product in a low-cost production time; it can also produce a wide range of materials. However, in the history of AM, wood was encompassed mainly in FDM techniques, where the wood fibers reinforce thermoplastic polymers, providing changes in mechanical properties and improving the end-of-life management [6]. Direct Printing (DP) as a filler in a polymer matrix is how GTR is now applied in AM, for now [7].



Figure 2.1: AM concrete wall [2]

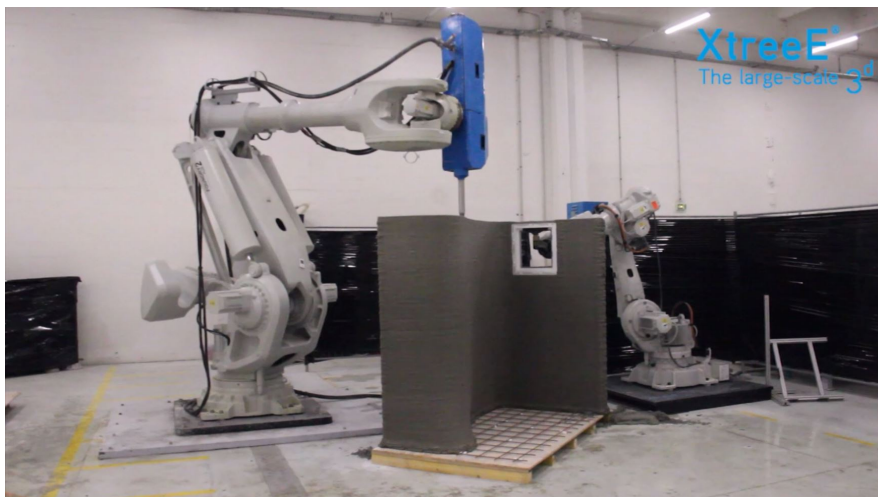


Figure 2.2: XtreeE System [3]



Figure 2.3: ProJet CJP 860Pro. Construction volume: 508 x 381 x 229 mm [5]



Figure 2.4: S-MAX Pro. Construction volume: 1800 x 1000 x 700 mm [1]

2.2 Binder Jet using natural materials

It is possible to use BJ technology to manufacture fibrous composites. A case study that uses gypsum-sisal fiber mixed with traditional raw material powder was analyzed for this project purpose [8]. In that case study, the gypsum-sisal fibers are separated by a 1 mm mesh size sieving and then mixed, at a 1% rate, with the powder for 10 minutes. That study concluded that it is possible to reinforce gypsum parts with natural sisal fiber. It gives the final part a greater strength (41%) since the parts with sisal end up having more pores. More pores mean making it more penetrable by the resin applied when post-processing. It gives the final part an increase in almost 60% of strength in the (y) direction (orientation that the fibers acquired when deposited along with the powder).

The following waste materials, such as wood flour, rice husk, and miscanthus fiber, were studied using BJ technology by Henning Zeidler [9]. The machined material has the density, water resistivity, biocompatibility, and mechanical properties that allow packaging for sensitive prototypes.

That paper presents research for a biodegradable easy to handle, readily available, and non-toxic binder. The Additive Manufacturing (AM) process, applied in ZCorp Z510, Z402, and Z310 BJ machine models, had to be altered to fit the conditioned biobased use fibers [9]. The binder requests do not fit the common 3D Printer binder properties. In the presented study, to overcome the material's inertia to react with known binders, solid binders were investigated and mixed with the powder before printing, making a "multimodal powder mixture". This solid binder reacts when in contact with an aqueous solution. The successful tests were lignin sulfonate, sodium silicate (waterglass) and polyvinyl alcohol, whereas the latter provided the best results. Still, compared with other AM technologies, like stereolithography (SLA) or Selective laser sintering (SLS), mechanical properties are shallow, so a post-treatment by infiltration or coating is needed.

Henning Zeidler uses acrylic resin, epoxy resin and stearin to infiltrate parts. Acrodur (high-performance, water-based acrylic binder), Polyvinyl Anime (PVA_m) (commercially available under the name Lupamin) were used as coating materials to change their mechanical properties. Applying epoxy resin infiltration achieves the best results in terms of compression strength, as seen in figure 2.5.

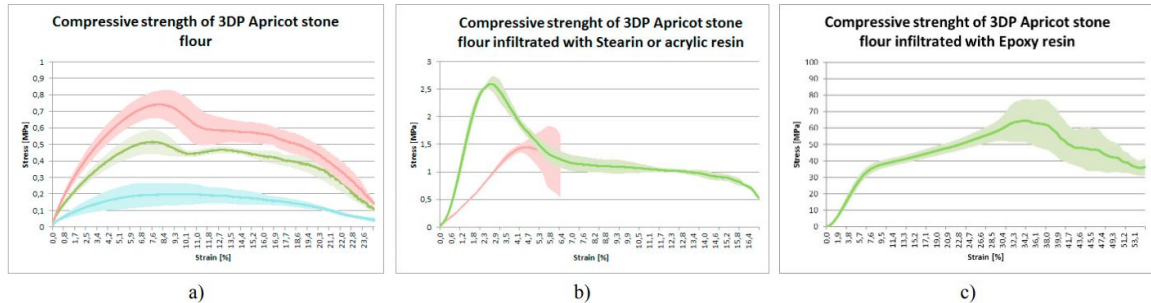


Figure 2.5: compressive strength a) Acrodur coated (red top); uncoated (green center); Lupamin coated (blue bottom) b) stearin (green top)

2.3 Binder Jet with powder mixtures

There is also the possibility to create a mixture of the two materials, wood and GTR. Traditional binders used in wood composite tend to create several environmental and mechanical problems. These binders are thermoset synthetic adhesives that create difficulties when trying to cut or saw the material. Most important for this paper, it decreases flexibility and damping performances. On the other hand, adding rubber units can solve these problems while giving a purpose for the rubber tires' end of life.

BJ with powder mixtures was studied to improve wood composites used for furniture, floorings, walls, and others [10]. A study made with 20 to 30 mm long, 10 to 150 mm wide, and 4 to 6 mm thick vaporized wood chips milled into fibers with measures of smaller than 0.15 mm (17%) to larger than 1.7 mm (18%) and Waste tire Powders (WTPs) with dimensions of 0.55 to 1.09 mm, was performed to create wood rubber composite panels. This overlaid wood-rubber composite (WRC) uses a 150% low molecular melamine-formaldehyde (MF) resin transparent layer on top, and the second layer contained 120% MF resin. The bottom layer was impregnated with Phenol formaldehyde resins (PF) with a dark yellow color. The WRC panel bonded with Urea-formaldehyde resin (UF) is the third layer right on top of the Kraft paper impregnated with PF resin. Tests were performed in specimens of 290 mm by 50 mm thickness parts off 100% wood fiber and composites of 10, 20, and 30%. Xinwu Xu [10] performed Flexibility tests in-thickness to conclude the performance in high energy absorption flooring environments like sports fields. Using a compressive load of 6 kN on a 100% wood fiber plate had an accumulated displacement of approximately 1 mm on the first load and 5 mm on the fourth load, as the composite using 30% rubber had an accumulated displacement of approximately 2 mm on the first load and 11 mm on the fourth load. The

thermoset resin used as a binder for the WRC panels by Xinwu Xu was UF resin, using Ammonium chloride (NH₄Cl) at 1 % level curing agent. The mixture of the two materials was three wood to one rubber ratio.

That research concluded that it is possible to modify wood fibers' strength and viscoelastic properties when adding recycled rubber. However, using this technique decreases mechanical properties. For example, the inner bond (IB) strength of a 100% wood Panel is 0.95 MPa, as the WRC panels with 10% rubber are 0.65 MPa. In any case, this project should not discard this possibility and perform tests to see if using the binder jetting technique could bring more positive information in combining these two materials. It could also be advantageous when creating the binder because it is possible to find an adhesive that only reacts with one of the materials trapping the other within the object while the machined part is fragile, not having the final treatment properties (meaning it is steel a green part).

2.4 Process development

To create this specific large-scale AM system with new materials and combinations will be considered the method suggested in the five steps used by Utela et al. [11].

2.4.1 Formulation of the powder

According to the project briefing, the PRINTbig project is developing methods to use materials seen as industrial waste. These materials can be tire pellets, grit, wood shavings, among others.

Fine powder has better advantages when pursuing detail in smooth surfaces, but can also complicate the process of 3D printing by forming agglomerates due to Van der Waal's attractive forces. These small particles also tend to stick to any other bodies, creating the machine's damaging parts. Their irregular shape can also increase friction lowering flowability. All these combined can cause an irregular layer spread and uneven densification [12].

There are very few limitations to the materials used in this system. As long as it is possible to formulate them into powder, the machine will adapt to the different powder properties. The choice of whether the powder should be wet or dry has lower importance than the size. Nevertheless, when using dry deposition, spherical powders work better than irregular shapes powders.

Additives can be added to the bulk material to affect the powder deposit ability, printing behavior, final part properties, and post-processing behavior. Stearic acid or derived stearates,

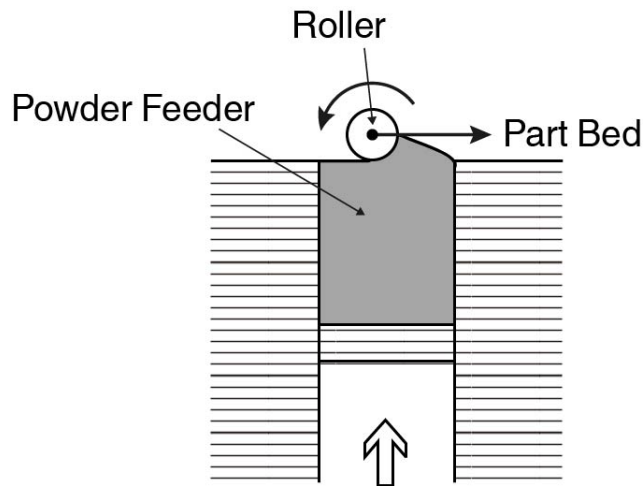


Figure 2.6: Counter-rotating roller

such as zinc or calcium stearate, are examples of lubricant materials to increase dry powder performance, in amounts of 1-2% by weight[13]. A commercially available SPAN 85 from Sigma Chemical Co., St. Louis, Mo., USA, and Lecithin can prevent distortions in printing. This printing aid prevents fine particles of the mixture from becoming airborne while dispensing fluid from the print head, which would distort the printed article [14]. Include fibers like Polymeric fiber, ceramic fiber, graphite fiber and fiberglass in the powder mix can increase dimensional stability [14]. This technique is significant for the project in development due to the dimensional aim.

Each spread layer is at least three particles thick in commercial machines due to powder flow and spreadability [12]. A standard dry powder deposition method is to use a counter-rotating roller (the roller direction at the bed surface opposes the travel direction, Figure 2.6). This roller deposits new layers of dust, leaving the previous layers undisturbed and also serves to push new powder in front of the roller as it traverses [14] [15]. Because the bed density directly affects the density of the green part, increasing the packing density of each deposited layer is often desirable. Dry powders can be compacted using mechanical vibration, acoustic energy, sonic/ultrasonic vibrations, or a piezoelectric scraper [16]. SLS investigations should also be considered; SLS also begins with a deposition of a thin layer of powder [17].

2.4.2 Selection of a binding method

Ben Utela researched nine different liquid binding methods for his study: organic liquids, in-bed adhesives, hydration systems, acid/base systems, inorganics, metal salts, solvents, phase-changing materials and sintering aids/inhibitors [11].

The use of liquid-binder can create clogging problems, potentially damaging parts of the machine and needing human assistance during prints. This fact will slow the process and

make it less reliable [14]. One way to solve this problem is to use binders that react after sprayed to minimize the risk of clogging inside the machine. Like the ProJet CJP 860Pro, some existing machines have an automated system that purges the binder after each layer. Purging the binder can keep the nozzles clean, preventing the binder from clogging and obstruct the outlet of material.

The binder selection affects the strength and porosity of the final part. In some cases, to make the printing process faster, a binder that needs secondary hand labor processes is required. This type of binder is known as "fugitive binder" [11]. A fugitive binder is a binder that holds the powder layer together to get the necessary strength to hold the final printed part. Meaning the part will be weak but can still safely transport and handle the raw piece into a secondary process that fortifies its final strength properties.

Since the PRINTbig project proposal aims at various powder materials, an organic liquid binder will be the most probable solution. The organic liquid binder is one of the most versatile binder methodologies. Examples of organic binders can be Butyral resins and Polymeric resins. Butyral resins, mostly used for strong bindings and optical clarity; its significant applications are laminated safety glass for automobile windshields [18]. Polymeric resins are resins based on Poly (styrenedivinylbenzene) resin manufacturing technology; these resins can adsorb organic compounds from aqueous solutions [19]. Industry uses this material in automobile-related components such as seat belts and carpets [20]. A subset of organic binders is preceramic polymers. They are used as reactive binders to produce technical ceramics and, also, to join advanced ceramic components [21].

Inorganic binders are also attractive to research for finishing purposes. A typical selection is colloidal silica due to its variety of uses and ease of manipulation [18].

2.4.3 Formulation of the liquid binder

The binder is an essential type of material that will be part of the final piece. This material is in charge of attaching the powder material. It has to have a reliable deposition through the print head. A liquid that only deposits sporadically is not useful for this type of technology. A rapid binder is preferred; every little time possible to withdraw from the binding process on each layer will make a big difference on a time-consuming level for the final piece, especially in this big product project. Some additions can be made in the binder to help reduce nozzle clogging [18]. Citric acid can be the right choice to regulate the pH [18] agents to increase viscosity can help to arrest droplet spreading.

Liquid rheology is important for the binder's reliability, and surface tension is the most important property to alter. Adding alcohol (like methyl alcohol) with water instead of adding only water can alter surface tension [12]. Still, a liquid's viscosity is also an important factor,

is more complicated than surface tension, and is affected by pH, solids loading, polymer loading and polymer length [11]. A liquid in the correct rheological ranges for the printhead and adequate rehydration and stability characteristics is suitable for test printing.

2.5 Literature Review Conclusions

It is essential to highlight that the manufactured printed parts aim for a maximum lifetime. Sometimes a concrete definition of that time is desirable when projecting a new object. Moreover, the binder, usually made of non-biodegradable materials, should follow up on the concept of renewable materials even though the main reason for this project is to reuse waste materials in applications with an extended lifetime. Thus the use of biodegradable resins is not advisable in this scope due to its short lifetime.

Not every study reveals test conclusions about the mechanical properties of the different materials studied but is relevant to point out the possibility of mixing different powders to test the alterations in the properties of the final parts and different types of post-treatment materials.

3 Experimental Materials and Procedures

To create the large scale BJ system, it was required to find a binder and formulate its deposition method. It was also assigned an adaption to the existing CNC machine available at the Center to Rapid and Sustainable Product Development, Polytechnic Institute of Leiria (CDRSP) installations.

3.1 Test plans

The following chapter will study the binder's formulation by its deposition behavior and its reaction to the dust material. The investigation will start by choosing three potential binder materials. Each binder will be released on the matrix material to examine its effect. The reaction will be studied by exposing the test to time and temperature.

Later, to approach a different printing method where the printing system joins the part by heat instead of binder drop, the matrix materials were premixed with the binders and exposed to temperature after the mixture was dried.

Then, having a material joining method consolidated, layers' creation was tested at a testing platform developed by CDRSP.

3.2 Materials and equipment

Dust of GTR and wood were supplied by CDRSP with the initial grum size up to 500 μm . These dust materials were separated into 100 μm , 200 μm , 300 μm , 400 μm , and 500 μm , then they were dried in a greenhouse at 50°C for one week to remove all humidity.

Having the matrix materials established by the project briefing, the following request is to obtain or design a suitable binder. The binder is responsible for holding the part together and give it enough stability to allow secondary treatments to the printed part without damaging its original form. It is also essential to have a low surface tension to avoid binder agglomeration

during the printing process.

The CDRSP provided a three-axis CNC machine programmed using edingCNC. This machine has a Z-axis that is a bed platform that moves up and down, and it has the axis Y and X that should draw the layer shape using the binder as ink. A counter-rotating roller, a nozzle, a deposit and a dust trimer had to be designed and adapted to the existing machine.

Test specimens are going to be printed, and the tensile properties are studied to analyze future applications.

3.3 Binder drop

Three different types of binders and four different types of dust material were chosen to perform a drooping test using a binder drop on the dust material, figure 3.1. The chosen binders were: Aquaseal, PVA, and Acrodur 950L. These are liquid binder that seems fit to perform in a binder jetting machine. The types of dust used for testing were two different grain sizes of two different materials: Two samples of dust wood with 400 μm and 100 μm grain size and two samples of WTR, having the test samples grains that vary between 100 μm to 400 μm and 500 μm to 800 μm .

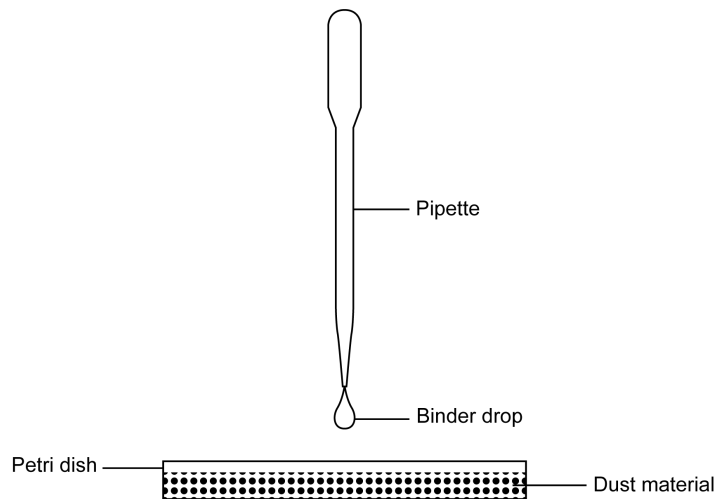


Figure 3.1: Scheme for binder tests

Acrylic binder “AQUASEAL” cures using heat. Use a heat source to cure the layer and experiment with different temperatures. This binder is supposed to cure at 100 °C. Acrodur 950 L resin (UV curing) as the possibility to mix with water and is supposed to cure with UV light, but in the technical sheet, it says it solidifies exposed to 120 °C for 2 hours. Polyvinyl Alcohol can dilute when mixed with water and heated. It can then be used by drying it with air (like glue).

According to these pre-known suppositions about the binders, a table was established

for each material with two variables: temperature in °C and time in minutes 3.2 3.3 3.4. The four different types of dust were put into different glass recipients. Drops of the binder were deposited on each material, and a stove was used to expose the experiment to different temperatures. The drops had an average diameter of 6 mm and penetrated an average of 3 mm, in less than 400 μm dust particles, and 4.5 mm, in particles with equal or more than 400 μm. Acrodur 950L was not considered due to its high viscosity making the drops bigger and not penetrating the dust, leaving the drop intact on top of the dust like a marble as seen in figure 3.5. An evaluation based on observations was made to every experiment to identify the best combination of grain size, binder material, temperature and time exposed to that temperature.

3.3.1 Aquaseal

The first binder tested was Aquaseal, a soluble binder in water. Tests were performed using temperature has a reactor component to hardener the binder. The temperatures tested were 80 °C, 100 °C and 120 °C, during 1, 10 and 30 minutes. Aquaseal does not react to any of these temperatures in one minute, it does not differ significantly, reactions between the same material with different grain sizes, and it found no difference in experiments of 100 °C and 120 °C. The binder impregnated and mixed better with the wood than it did with the tire. However, the first 10 minutes exposed to any of these high temperatures, the dropping could be considered green or pre-bonded and move to a second phase of the process, like finishing with a stronger binder. Still, the rubber mix presented much more flexibility than the wood mix. The wood composite recorded its best properties when exposed to 100 °C for 30 min. However, the material probably does not have the mechanical properties needed for this technology when exposed to stress situations. The tire composite presented is had the best performance at 100 °C at 10 minutes, but it performed a bit poor since it unleashes rubber grains when managed (figure 3.2).

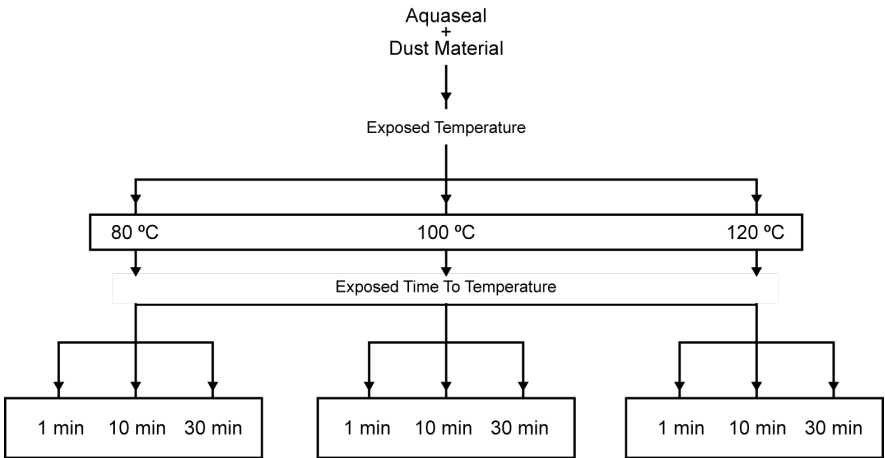


Figure 3.2: Aquaseal temperature tests

This introduction of the binder aquaseal to the project created the possibility to test the

material to be cured using a heater that actuates directly on the layer, having the suggestion that it should be mixed with the dust material and dried so that the dust would not agglomerate. Testing this binder and exposing the powder and binder mixture at 80 °C for 10 minutes, resulting in the evaporation of all the water from the binder. However, it did not cure, making it very easy to separate the grains, concluding that this idea should come to study in the next stage of testing.

3.3.2 PVA

The second binder test was Polyvinyl Alcohol (PVA) in liquid form. Usually, this binder is a release agent or used as glue for the artists that create their paint. It is a water-soluble synthetic polymer. It reacts at room temperatures (RT), but tests with controlled high temperatures were performed to accelerate and improve the process. So, RT, 50 °C and 70 °C, during 10, 20 and 30 minutes, were the base values to perform the test on this material. This binder was very ineffective with the 400 µm wood, not giving the material any strength at RT and very little with the increase of temperature. It was found that the binder is very ineffective at RT, but with the increase of temperature, it performs better than the aquaseal. It is possible to observe a big difference between the two different grain sizes of wood, but when working with the rubber grains, the results were very similar between them. After performing PVA tests, this study concluded that to create a decent green part to handle and move to a post-processing stage may be enough to have a small grain size wood or any of the two types of rubber and expose them (binder and dust) during 10 minutes to 70°C (figure 3.3).

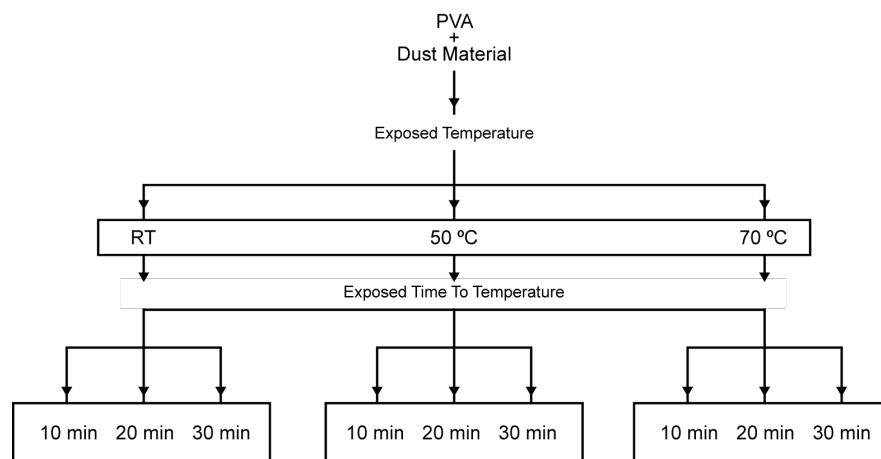


Figure 3.3: Polyvinyl Alcohol temperature tests

3.3.3 Acrodur 950L

Acrodur drop was too viscous and did not impregnate with the dust material, making it impossible to use in this kind of process (figure 3.5).

These tests present a different path for each binder used. The next testing stage will use some shapes in layer thick dust size to make conclusions about the definition and control off the binder's drop. Acrodur resin will no longer be used for testing phases (figure 3.4).

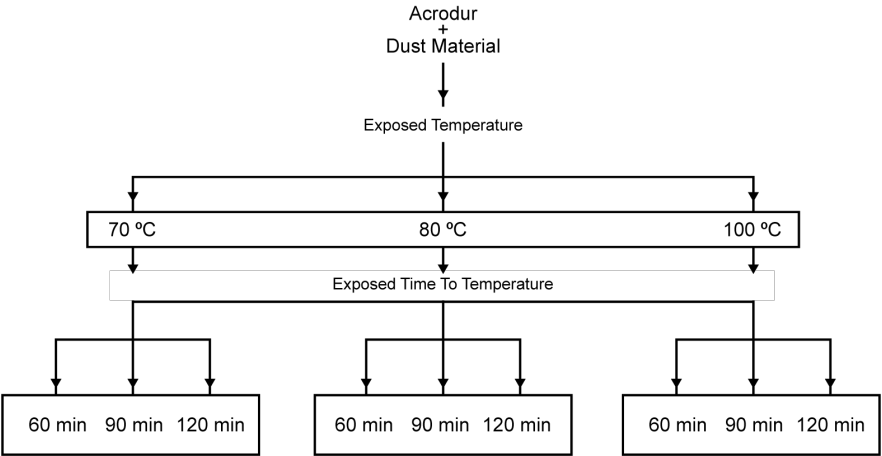


Figure 3.4: Acrodur 950L temperature tests

3.4 Binder coating

As previously concluded (point 3.2.1), it was noticed that it could be possible to dry the Aquaseal on the dust material and separate the dust particles when the binder was exposed to 80 °C for 10 minutes. So, some tests were performed to find a possibility to mix the materials, keeping the mixture (dust) free to be manipulated by the machining system and use heat to bind the binder in specific points of the layer. Mixtures of 30%, 50% and 70% of Aquaseal Binder were used with the dust materials. The quantities used are shown on the tables 3.1, 3.2 and 3.3 referenced by weight. The final result is supposed to become a solid material, so the mixtures were poured in silicone molds with the shape of test pieces (figure 3.6). This way, the parts would be easy to remove and analyze after hardening.

The 30% binder mixture was the first test to be performed. The results were very negative comparing with the expected, the composite did not solidify properly, and large grumps were agglomerated, (figure 3.7). The 50% binder mixture had better results on wood, but it worsened the results on WTP (figure 3.8). The 70% binder mixture absorbed the dust materials,



Figure 3.5: Acrodur drop. As it can be observed, the binder material did no impregnated the dust.

Dust Material	Dust Weight (g)	30% Aquaseal Weight (g)
400 μm Wood	5.42	2.32
100 μm Wood	3.78	1.62
500 μm - 800 μm WTP	9.41	4.03
100 μm - 400 μm WTP	9.16	3.93

Table 3.1: Wood and waste tire powders (WTP) materials weight mixture with 30% Aquaseal ratio.

Dust Material	Dust Weight (g)	50% Aquaseal Weight (g)
400 μm Wood	2.95	2.95
100 μm Wood	3.22	3.22
500 μm - 800 μm WTP	8.43	8.43
100 μm - 400 μm WTP	6.14	6.14

Table 3.2: Wood and waste tire powders (WTP) materials weight mixture with 50% Aquaseal ratio.

Dust Material	Dust Weight (g)	70% Aquaseal Weight (g)
400 μm Wood	1.27	2.96
100 μm Wood	2.37	5.53
500 μm - 800 μm WTP	4.73	11.03
100 μm - 400 μm WTP	6.81	15.89

Table 3.3: Wood and waste tire powders (WTP) materials weight mixture with 70% Aquaseal ratio.



Figure 3.6: Test pieces silicon molds. The moulds contain 100 μm of wood, 100 μm to 400 μm of waste tire powders (WTP) and 400 μm of wood (respectively) with a 30% aquaseal binder ratio.

sequentially not allowing the mixture to disjoint into dust (figure 3.9).



Figure 3.7: Results (from left to right) 100 μm - 400 μm WTP, 400 μm wood, 500 μm - 800 μm waste tire powders (WTP) and 100 μm wood with 30% binder ratio.



Figure 3.8: Results (from left to right) 100 μm wood, 100 μm - 400 μm WTP, 500 μm - 800 μm WTP and 400 μm wood with 50% binder ratio. WTP- waste tire powders



Figure 3.9: Results (from left to right) 100 μm - 400 μm WTP, 500 μm - 800 μm WTP, 100 μm wood and 400 μm wood with 70% binder ratio. WTP- waste tire powders

3.5 Layer Experiments

After testing which binders fit the requirements for creating parts using this BJ process, the next step is the creation of layers. A testing platform was designed at CDRSP to test dust layers to create shapes, mimicking the BJ process (figure 3.10). Because the binders will need heat and the testing platform cannot create predefined temperatures, the layers' base is cardboard (figure 3.11), so it is possible to remove the part and move it to a heated oven to finish the process without damaging the raw material.



Figure 3.10: Testing platform. Source: CDRSP - Center to Rapid and Sustainable Product Development, Polytechnic Institute of Leiria, Portugal

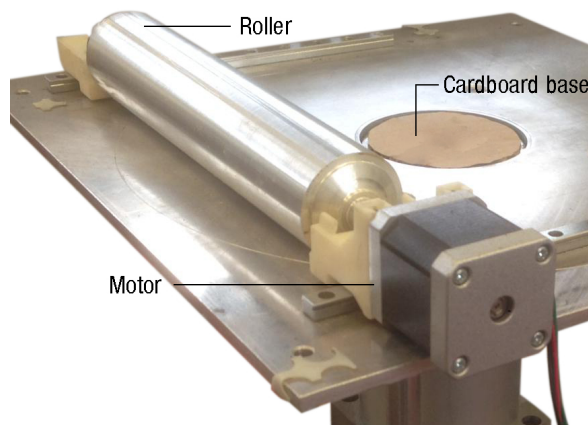


Figure 3.11: Testing platform. Source: CDRSP - Center to Rapid and Sustainable Product Development, Polytechnic Institute of Leiria, Portugal

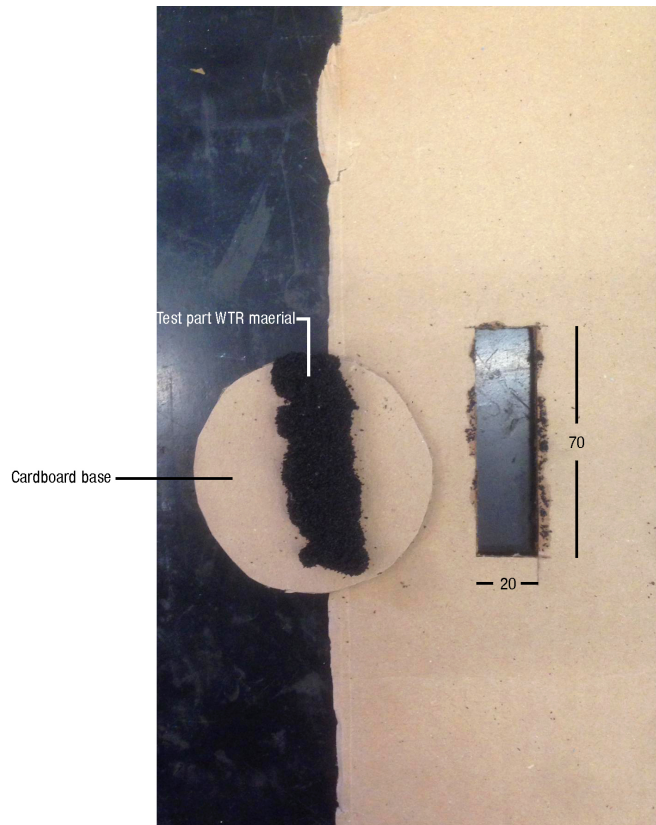


Figure 3.12: Mask to delimit binder drop area.

The shape intended is a rectangular parallelepiped shaped object in order to perform posterior mechanical tests. The rectangular parallelepiped dimension horizontally builds 70 x 20 x 3 mm due to the testing platform dimensions. To create the 70 x 20 mm rectangular shape layer, the binder was spread on top of the dust layer previously created, and a cardboard mask delimited the area to spread the binders (figure 3.12).

3.5.1 Testing Platform

In order to perform small tests with binders, a machine was developed previously at CDRSP, this testing platform enables the creation of layers without spending large quantities of dust material. This machine consists of a cylindrical build base, with a cylindrical elevation system to mimic the z-axis, seen in figure 3.13 as the green part, and a roll to spread the dust through the build platform.

3.5.2 Polyvinyl alcohol Tests

After deposition, the PVA binder successfully impregnated the dust matrix material. Then, the printed part was taken to a furnace at 50°C for ten hours to dry. The manufactured

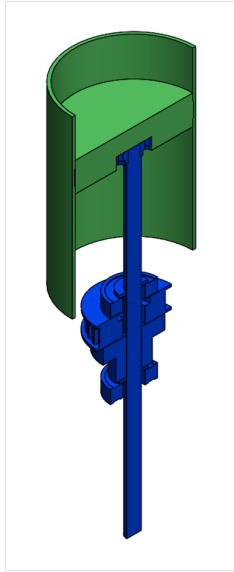


Figure 3.13: Cylindrical elevation system. The green parts are the build base and the extreme walls of the construction build, the blue components are the mechanical parts that create the vertical movement. Source: CDRSP - Center to Rapid and Sustainable Product Development, Polytechnic Institute of Leiria, Portugal

parallelepiped presented the possibility of testing properties for a green part. 12 test samples of each material (WTR and wood) were made, and six of each material were infiltrated with cyanoacrylate to test possible mechanical strength improvements.

It was also noticed that the binder took 24 hours to dry at RT.

PVA tire

The tests using GTR without giving it a post-process infiltrated with cyanoacrylate (table 3.4) presented results with high variability (percentual standard deviation (PSD) > 30%): 42.6% for the yield strength and 36.8% for the tensile strength values. It is possible to observe in Table 3.4 that Test 4 had exceptional high results, both at yield strength and tensile strength, making this test specimen the principal responsible for the high PSD values. In any case, the PSD value without the specimen for Test 4 does not have significant results (35.6% in yield strength and 30.4% in ultimate tensile strength); however, as the PSD of either one is above 30%, there is significant variability and vast dispersion of the data. Therefore, this high PSD means that there are a considerable variability within the values obtained in the different tests.

Sample PVA tire	Area (mm ²)	σ_y (MPa)	UTS (MPa)
Test 1	153	7,05E-03	8,49E-03
Test 2	100	8,75E-03	1,00E-02
Test 3	94,5	1,48E-02	1,46E-02
Test 4	100	2,28E-02	2,40E-02
Test 5	88	1,19E-02	1,56E-02
Test 6	77	1,75E-02	1,82E-02
PSD	-	0.43	0.37

Table 3.4: Ground tire waste (GTR) coated with polyvinyl alcohol (PVA) test samples tensile properties table

Sample PVA wood	Area (mm ²)	σ_y (MPa)	UTS (MPa)
Test 1	84	2,98E-03	7,74E-03
Test 2	110	2,94E-03	5,91E-03
Test 3	126	3,17E-03	5,75E-03
Test 4	148,5	1,18E-03	2,36E-03
Test 5	126	1,98E-03	4,17E-03
PSD	-	0.35	0.39

Table 3.5: Dust wood soaked with polyvinyl alcohol (PVA) test samples tensile properties table

Polyvinyl alcohol wood

The tests realized with dust wood soaked with PVA presented the lowest deviation of all the tests, but when comparing to the standard value (30 %) it is higher (34.6 % in yield strength and 39 % in ultimate tensile strength). If the fourth test is removed, the values' dispersion is within the target (19.3 % in yield stress and 24.8 % in ultimate tensile strength) (Table 3.5).

Polyvinyl alcohol wood with cyanoacrylate finish

When testing with PVA wood with cyanoacrylate finish, the machine might have some problems with test 4 because negative force values were obtained. Therefore it was not considered in the study. Two samples broke during the process and could not be tested, leaving only four tests. The first test had results far below expectations, and the PSD was very high (78.9 %) in yield strength and higher (70.1 %) in ultimate tensile strength. Without the first test, the PSD of the yield stress of the second and third tests drops to 10 %, leaving, even then, high variability in the ultimate tensile strength (39.6 %) (table 3.6).

Polyvinyl alcohol tire with cyanoacrylate finish

The results obtained with PVA tire with cyanoacrylate finish showed a too high values dispersion, with a percentual standard deviation of 67.3 % in yield strength and 76.1 % in ultimate tensile strength. Even when removing the first test values, which are considerably lower than

Sample PVA wood cyanoacrylate finish	Area (mm ²)	σ_y (MPa)	UTS (MPa)
Test 1	126	1,5E-01	4,29E-01
Test 2	150	1,65	4,42
Test 3	138	6,77E-01	1,85
Test 5	162	6,91E-01	2,95
PSD	-	0.79	0.7

Table 3.6: Dust Wood soaked with polyvinyl alcohol (PVA) and cyanoacrylate test samples tensile properties table

Sample PVA tire cyanoacrylate finish	Area (mm ²)	σ_y (MPa)	UTS (MPa)
Test 1	154	1,40E-01	2,40E-01
Test 2	165	8,97E-01	1,75
Test 3	135	7,78E-01	9,85E-01
PSD	-	0.67	0.76

Table 3.7: Ground Tire Waste (GTR) soaked with polyvinyl alcohol (PVA) and cyanoacrylate test samples tensile properties table

the remaining values, there is a high variation of 55.4 % and 42 % in the yield stress and the rupture stress, respectively (table 3.7).

3.5.3 Aquaseal Tests

Aquaseal tests failed to impregnate the dust enough for the roll to spread the layer above, making it not to be an appropriate binder to use in this technique (Figure 3.14).



Figure 3.14: Aquaseal drops on a layer of 200 μm particle size wood dust.

4 Equipment

After concluding what materials and how these materials will be used, the project proceeded to a more physical phase, the mechanical machine's construction started with the construction of a method to spread the dust material to form layers. Later, a dust trimmer was projected to catch the leftover material pushed out of the machine perimeter.

Once the layer creation was established and controlled, Binder deposition techniques were tested with two different methods: one that pumps the binder and the other that drops it through gravity.

The software programming was then studied to test the machine's system and produce test specimens to examine the material properties.

4.1 Counter-rotating roller

The standard dry powder deposition method uses a counter-rotating roller to deposit new dust layers, leaving the previous layers undisturbed. It also serves to push new powder in front of the roller as it traverses. After the nozzle deposits the binder in each layer, additional dust is added to the system, and the roller function is to spread it on the build platform to create a new layer.

To create the roller system the following components were used: a stepper motor, a stainless steel tube 60.30 x 2 mm and 800 mm long, two bearings (one at each end of the tube), and two sets of Polylactic acid (PLA) 3D printed parts that secure the system to the machine and allow height adjustments (figure 4.1)

4.2 Dust trimmer

To form layers, it is necessary to add dust material to the system. The quantity of dust added needs no overthrow the exact quantity needed to make sure the layer covers the whole printing area in one single passage. This technique can save time and improve quality but creates a new problem; after each roller passage, the system throws out waste dust material

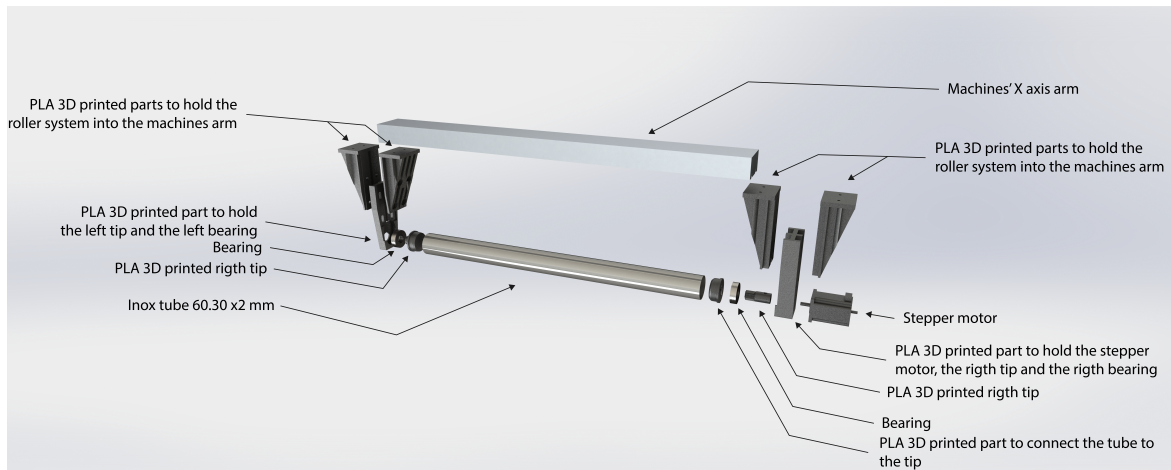


Figure 4.1: Counter-rotating roller parts.

from the printing area. A dust trimmer was created to catch the leftover dust, avoid waste, and avoid contaminating the machine's area.

4.3 Binder deposition

Commercially available, BJ Machines transfer the binder to the matrix material through 2D printing machines printheads. These printheads provide a controlled deposition required for detailed small parts and an intricate technique already mastered by the industry.

For this research purpose, a printhead is not available to reprogram. So two different types of binder deposition techniques are considered: a peristaltic pump is used to inject the binder, and a solenoid actuated valve to enable binder deposition through gravity.

4.3.1 Peristaltic pump

Peristaltic pumps are equipment used to transfer fluids under a specific flow. A complete peristaltic pump system consists of three parts: the drive, the head, and the hose. The primary and peculiar characteristic of peristaltic pumps is that the pumped liquid does not come into contact with any part of the laboratory equipment itself. The fluid comes into contact only with the hose's inner surface for the peristaltic pump, which does not damage the fluid and prevents contamination.

The peristaltic pump used for tests (figure 4.3) injects 1 ml of binder each turn. When inserted 5 volts of power, the pump takes seven seconds to make ten turns (1,43 turns/second), meaning the pump injects 1,43 ml/s of PVA binder.

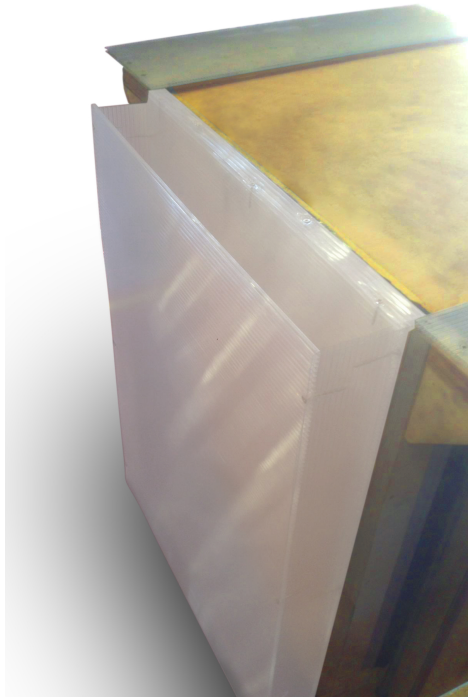


Figure 4.2: Dust trimmer box made out of corriboard.

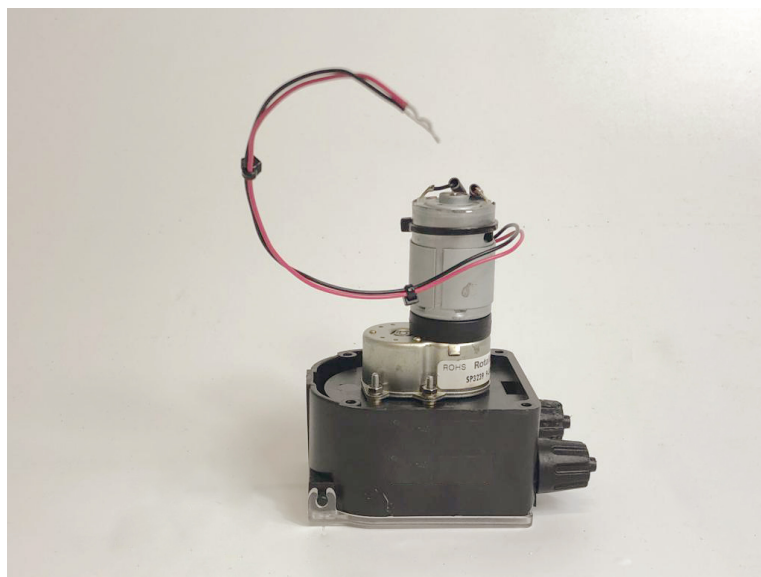


Figure 4.3: Peristaltic pump

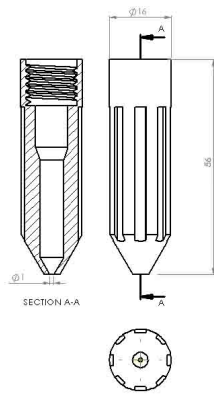


Figure 4.4: 1 mm nozzle.

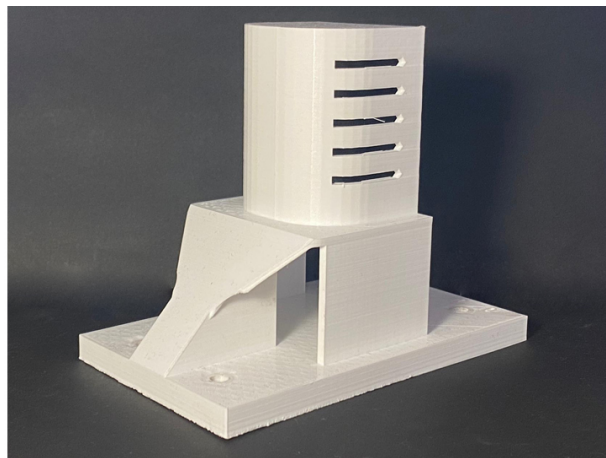
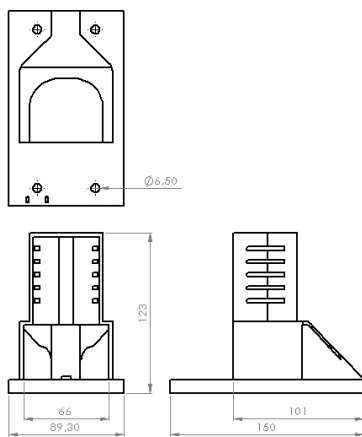


Figure 4.5: Support to hold the peristaltic pump.

For the first tests performed, a peristaltic pump was used. To this purpose, 20 parts were 3D modeled using CAD software and printed using FDM technology.

The first two parts designed were the support to hold the pump (figure 4.5) into position and a nozzle with a 1-millimeter diameter (figure 4.4). The peristaltic pump connects to a deposit (figure 4.6) supported above the binder extruder end. The deposit support was designed to allow the deposit to fit on top like a domestic water dispenser deposit (figure 4.7).

A hose adapter and a hose brake were designed to replace the original bottle cover (figures 4.8 4.9) to allow the binder to flow to the hose, and a hole was then cut on the deposit top to allow refilling and air flowability. A cover was then designed and printed (figure 4.10), not allowing the binder to spill during print. This cover leaves a hole on the top to allow air flowability. After this setup was assembled and tested, there was still a problem that had to be solved. The nozzle was not stable enough, so with the irregular pressure from the peristaltic pump, it had small dislocations during binder injection. It was modeled and printed a stabilizer that holds the nozzle to the machines' arm, not allowing small deviations (figure 4.11).

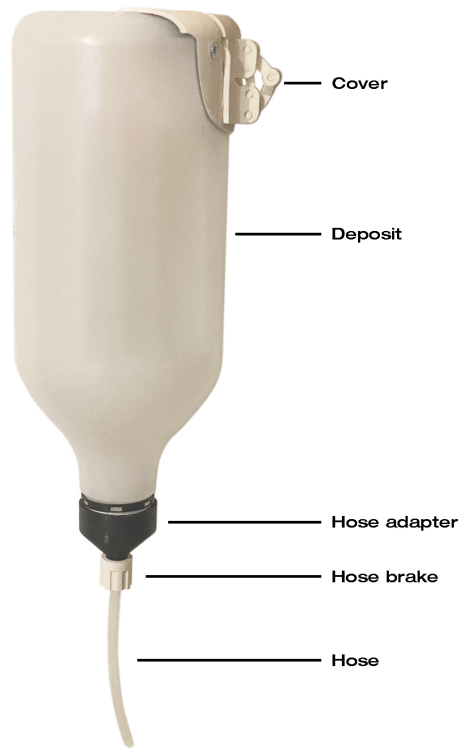


Figure 4.6: Two liter binder deposit.

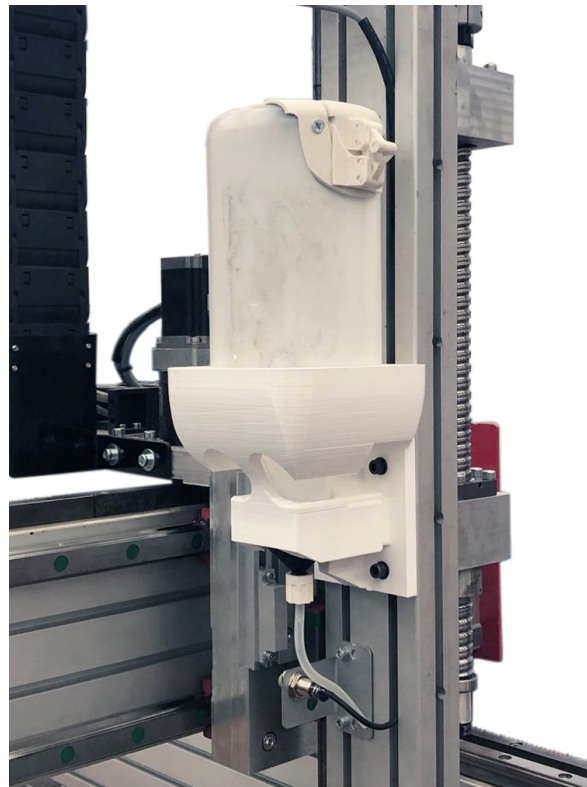


Figure 4.7: Deposit support attached to printer arm.

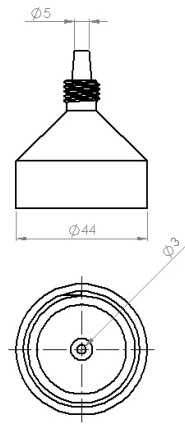


Figure 4.8: Hose adapter.

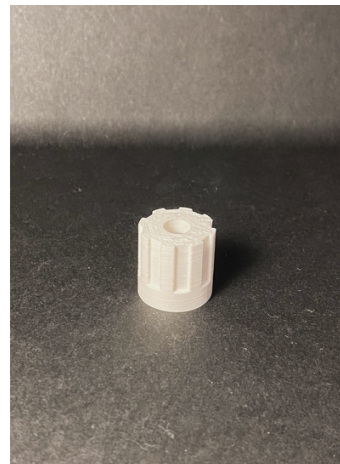
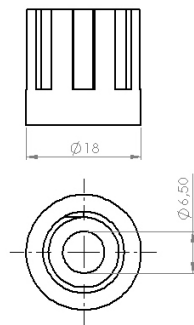


Figure 4.9: Hose brake.

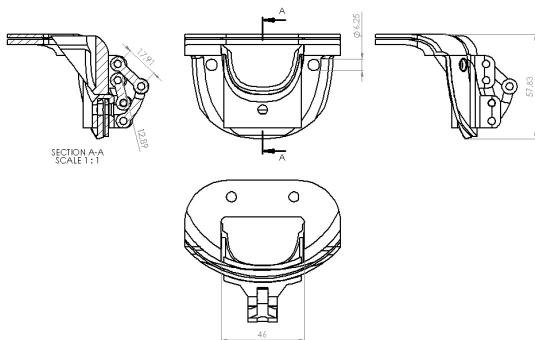


Figure 4.10: Deposit cover.

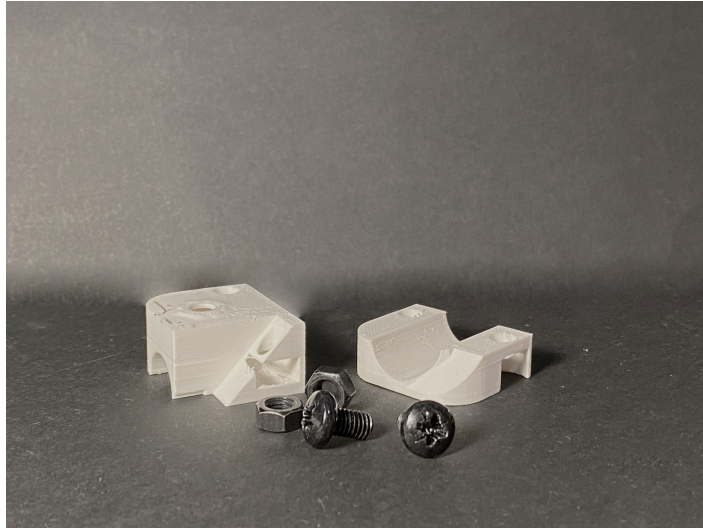


Figure 4.11: Nozzle stabilizer and the bolts and nuts to assemble it to the nozzle.

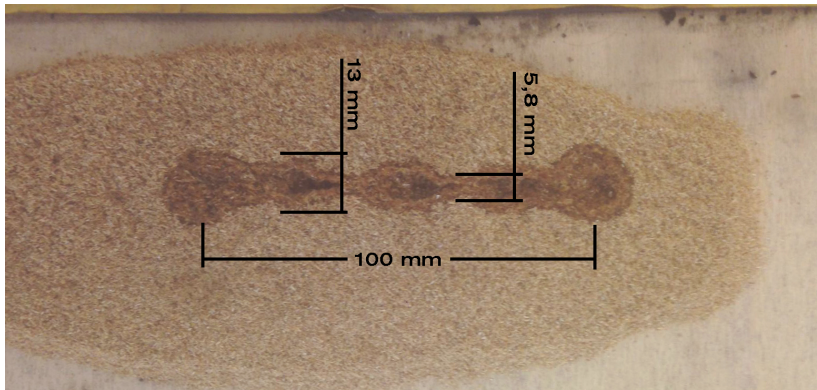


Figure 4.12: PVA line on the wood dust layer injected with a peristaltic pump through a 1 mm nozzle.

With all parts assembled and ready to be utilized, the study proceeded to the printer. A 100 mm line along the y-axis was injected to test binder flowability and impregnation at the maximum machine speed (0.386 cm/s). The results, as seen in the picture 4.12, the binder had a 5,5 mm penetration through the dust material, the line was irregular, the thickest parts had 13 mm, and the thinnest had 5,8 mm. Also, the injected binder created a fissure on the dust material due to exceeding pressure.

To fix the fissure problem seen in figure 4.12, a new nozzle with a 6,15 mm diameter tip (figure 4.13) was printed and installed to allow better binder flowability, solving the exceeding pressure problem. The measure added to the nozzle tip was decided to match the connecting tube's inner diameter. The result can be observed in figure 4.14. The fissure problem was solved using this technique, but there was an apparent flowability stabilization problem due to the mechanism used to pump the binder. After this last test, the peristaltic pump was discarded and a new technique was tested using the gravity strength instead of mechanically pump the binder through the nozzle.

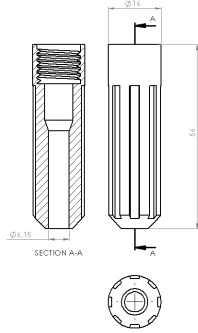


Figure 4.13: 6,15 mm diameter nozzle.

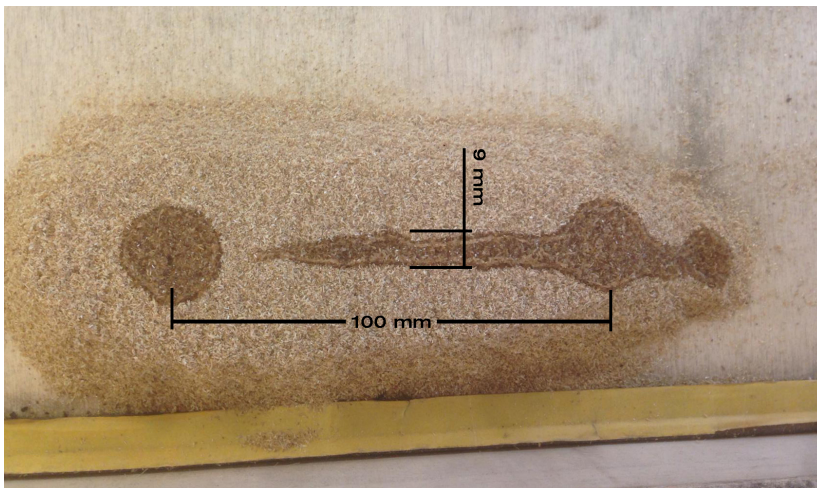


Figure 4.14: Polyvinyl alcohol line on the wood dust layer injected with a peristaltic pump through a 6,15 mm nozzle.

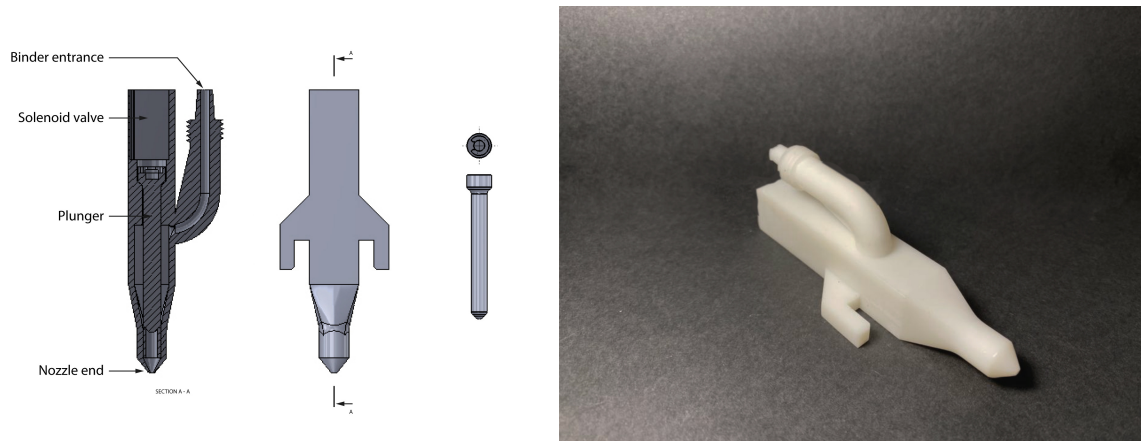


Figure 4.15: Image on the left: - Direct acting solenoid valve components. Image on the right: - SLA 3D printed solenoid valve with white resin.

4.3.2 Solenoid valve

A solenoid valve is a two-component electromechanically-operated valve that consists of an inductive coil encompassing an iron core at the center (plunger). When current flows through the solenoid, the coil is energized and generates a magnetic field pulling the plunger and overcoming the opposite force, in this case, the spring force. With this technique, the primary objective is to use gravity to pull the binder and a Solenoid powered plunger to control the deposition.

Solenoid valve 5VDC

The first attempt using this technique was made using a 5V Solenoid valve. To this purpose, a 3D model was created and 3D printed, as seen in the figure 4.15. Once again, the CAD software used was Solidworks, and the 3D printing technology used was Stereolithography (SLA) due to the essential details and tight tolerances.

This first attempt to use a solenoid valve was unsuccessful due to printing tolerances and mechanics. The liquid binder could slip through the electrical components creating the possibility to damage the solenoid parts. The plunger could also not isolate the nozzle end properly, not allowing a full stop to the liquid binder flow.

Solenoid valve 12VDC

The second attempt to use this technique was made using a solenoid 12VDC 1,86N 14mm 2,4W and an already used design available at CDRSP installations. This design had a plastic fluid precision blunt needle dispense tip (PFPBNDT) housing. The CDRSP installations also

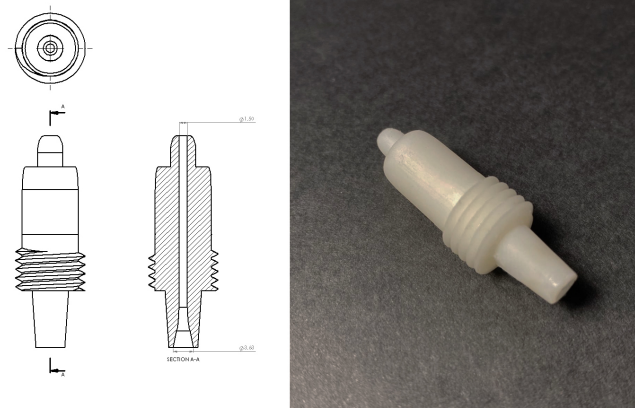


Figure 4.16: Valve connector. SLA printed part to connect the deposit tube to the solenoid valve system.

had available four different internal diameter PFPBNDT for testing: - 0.2, 0.3, 0.8, and 1.6 mm.

Two new parts were printed in order to perform the tests. One element was designed to fix the solenoid valve system to the machine; this part was printed in PLA using FDM technology. The second element was designed to connect the deposit tube to the solenoid system (valve connector); this part was printed in resin using SLA technology (figure 4.16).

Valve connector

The deposition system was not working correctly due to a valve connector design flaw. The binder flowed slowly through the valve system, causing the liquid to drain in discontinuous drops instead of falling as a continuous flow. These results created similar problems to the ones created before when using a peristaltic pump.

The part connected to the deposit tube and the solenoid valve system was removed to analyze the problem. The binder was then released through that connector without passing through the solenoid valve system. This experiment concluded that the liquid was draining in discontinuous drops when passing through the connector, assuming that the loss of pressure happened due to the connector's small internal diameter (1.50 mm) (figure 4.16).

The connector design was improved to allow the binder to flow continuously without losing pressure. This new improved connector had an interior hollow of 3.63 mm diameter. This change allowed the binder to flow without interruptions through the connector. After this alteration to the connector design, the PFPBNDTs with the smaller diameters were still draining discontinuous drops. So the only PFPBNDT accepted to create further analyses was the PFPBNDT with a 1.6 mm inner diameter.

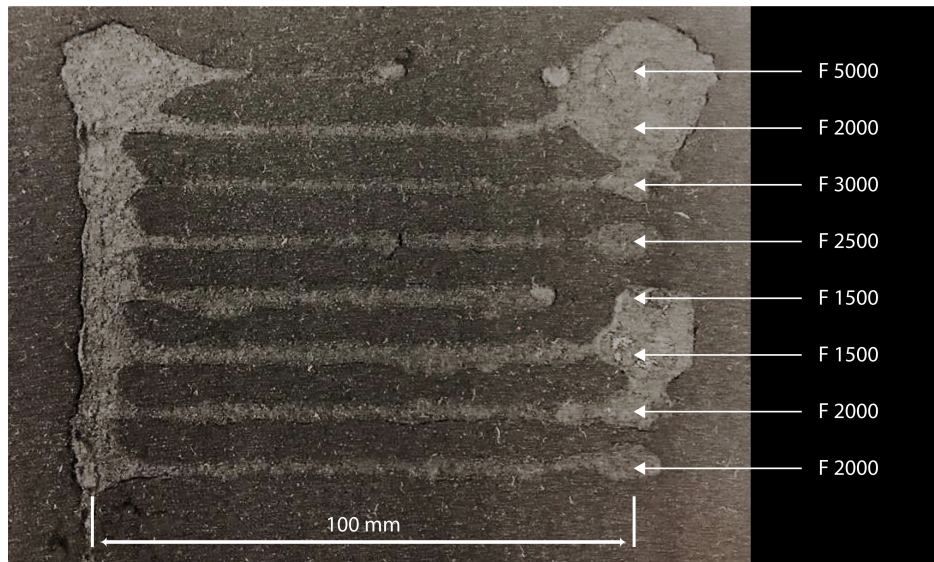


Figure 4.17: Bender deposition speed test.

4.3.3 Deposition parameters

After producing a deposition method and installed it at the printing machine, the deposition parameters were analyzed and defined to generate the most suitable layer conditions.

The experiment intended to estimate the time each PFPBNDT took to drop 10 ml of PVA. To perform this experiment, a 100 ml glass beaker filled to the 20 ml line by hand was used to then the binder be released through the system to fill it to the 30 ml line while counting the time it took.

The PFPBNDT with a 1.6 mm inner diameter took 90 seconds to drop 10 ml of liquid PVA. Meaning the system's flow rate using a 1.6 mm inner diameter PFPBNDT is nine milliliters per second (0.11 ml/s) of continuous flow.

100-millimeter lines of the binder were deposited on a WTR dust layer using different speeds: 4, 3, 2.5, 2 and 1 mm/s. The best result was obtained when the nozzle traveled at 2 mm/s. The bound line has a 2 mm penetration through the dust and is 5 mm thick when traveling at an optimum speed (2 mm/s) (figure 4.17).

4.4 CNC software parameters

After optimizing the deposition method and layer spreading, defining how the machine will perform is possible. Still, some adaptations will be necessary during this process.

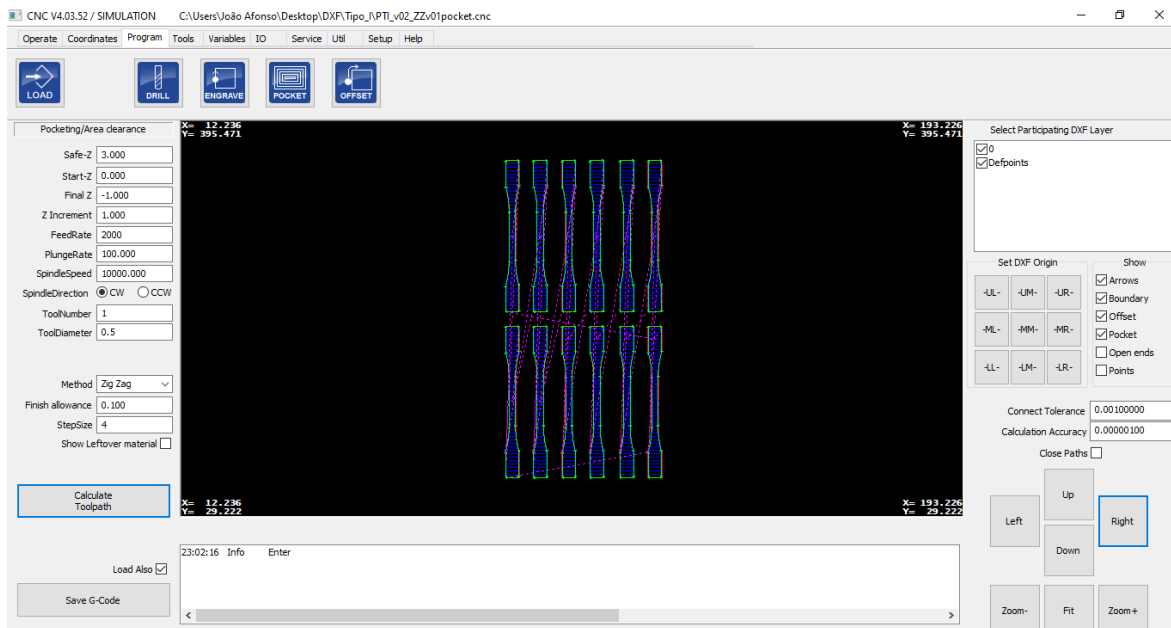


Figure 4.18: EdingCNC program interface.

4.4.1 Creation of the Gcode

The Gcodes were created using the edingCNC software. For this purpose, a DXF file of 12 2D test specimens was created in DraftSight CAD software. The DXF file was then loaded into the edingCNC program. This program is defined as subtraction manufacture machining, so some definitions must be adjusted for printing purposes.

The program interface can define the Z-axis position, the printing speed / Feed rate, and the printing method. The Z-axis position defines the height of the printing bed during binder deposition. The Feed rate defines the axes' movement speed; for this project, it was concluded that the best binder deposition speed was 2 mm/s. The printing method determines the nozzle path to cover the parts layer; the nozzle can path in a spiral or zigzag through the layer. Another relevant definition is the tool diameter; the tool diameter defines the spacing between lines and corner diameters (figure 4.18).

Because this software's programming possibilities are narrow, it is also possible to introduce operations directly on the Gcode file.

4.4.2 Material addition

To start the printing process, the machine, as all CNC machines, homes all axes. Once all axes are set and active, the X-axis requires to travel to the opposite side of the dust trimer to allow material deposition. The material deposition method was not automatized to this project execution, so a manual deposition needs to occur. The manual deposition is executed by

loading the necessary amount of dust material in the printing bed to satisfy the layer volume. Customarily, this value is overcome to guarantee that the layer is formed completely.

4.4.3 Layer creation

While the binder is being deposited, the roller is rotating to position 6000; this is relevant because when the layer is formed, the roller is counter-rotating back into position 0. For the roller to spread a layer of dust, it needs the X-axis to run transversal to the machine; simultaneously, the roller rotates in the opposite direction to the path taken. Each time a layer is created, the Z-axis needs to move down the same distance as the layer thickness, and the process of adding material and creating the layer repeats itself.

4.4.4 Binder deposition

The binder deposition process is done through the nozzle (figure 4.19). The nozzle moves within the X and Y axes' actions at the speed of 2 mm/s. The solenoid valve should be activated only when the axis is producing the parts layer and deactivates in the spaces between parts. This process should be programmed and automatized. The lines stay 4 mm distant between them to overlap 0,5 millimeters, ensuring layer filling.



Figure 4.19: Binder deposition.

After the layer is completed, the X-axis must go back to the opposite direction from the dust trimer, and the Z-axis goes down 2 mm. Then more powder is deposited manually, and the process is repeated.

4.4.5 Ground tire rubber testing

The system was tested using 200 μm GTR dust size provided by CDRSP at RT. Two examples of binder deposition methods were tested and their results evaluated.

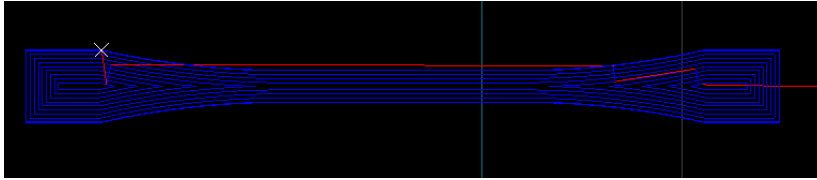


Figure 4.20: Spiral path.

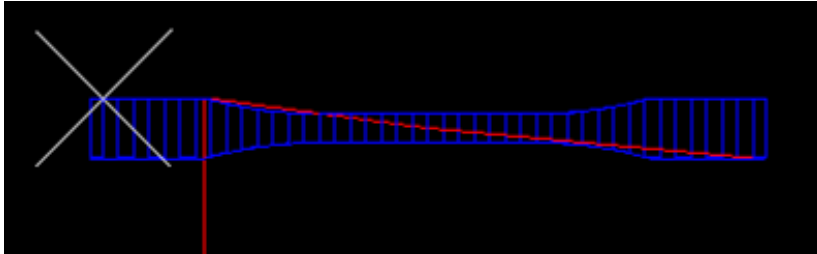


Figure 4.21: Zigzag path.

Spiral method

In the first attempt at printing the test specimens, the surface tension between the PVA binder and the GTR material proved an obstacle. The lines tended to attach, deforming the layer drawing. For this reason, it was impossible to use the spiral method. The lines created the part contour regularly, but once the nozzle starts depositing inside the contour, the binder would automatically move to the sides, leaving a hollow space inside the part and excess binder on the walls of the part (figure 4.20).

The binder was deposited manually in the center of the part's layers to correct this error and validate the test specimens for further testing. This method was performed in between the layer change process using a pipette.

Zigzag method

The zigzag technique was also tested (figure 4.21), attempting to bypass the binder accumulation mentioned. The program edingCNC generated a gcode that would zigzag the layer's interior and, afterward, draw the parts' exterior contour. This method did not work because despite the zigzag successfully depositing the binder on the parts infill, the parts' walls deposition would attach to the infill leaving just an irregular shape in the part's layers. The reverse was also tested, the nozzle would first draw the parts' contour and afterward deposit the infill, but a similar error happened to the spiral method failure.

So a mixture of the two processes was performed with a small layer between them. This means the Gcode had to be manually manipulated to adapt the printing system to these conditions. In the first layer, the specimens were only bound in the contours. Then a new

layer with 0,5 millimeters high was created to cover the first one. On top of this layer, the test specimens infill was printed. Next, the process repeated, but instead of a 2 millimeter, it was added a 1,5 millimeter layer.

5 Results

The first result was to conclude that the PVA has the right properties to be the binder used. It successfully impregnated the dust matrix material and created a decent green part to handle and move to a post-processing stage. It was also concluded that cyanoacrylate could be used as a post-process infiltrator to improve the printed objects' mechanical properties increasingly.

Then, having all the research about the technology and the binding techniques, the physical machine was developed. The creation of the Counter-rotating roller was the first component to be created. It was developed using a stepper motor, a stainless steel tube 60.30 x 2 mm and 800 mm long, two bearings (one at each end of the tube), and two sets of Polylactic acid (PLA) 3D printed parts that secure the system to the machine and allow height adjustments.

The second created component was created thinking about the reuse of the excess material. A dust trimer was created to catch the leftover dust, avoid waste, and avoid contaminating the machine's area.

A two-liter bottle was reused to serve as a binder deposit. A hose adapter, a hose brake, a deposit cover, and a deposit holder were successfully created to design this adaptation.

After producing a deposition method and installed it at the printing machine, the deposition parameters were analyzed and defined to generate the most suitable layer conditions. The bound line has a 2 mm penetration through the dust and is 5 mm thick when traveling at an optimum speed (2 mm/s).

In the deposit, it was installed a hose to connect it to the machine's nozzle. A solenoid valve 12VDC system was utilized to control the binder deposition with a 1.6 mm nozzle on the system tip to finalize the machine hardware (figure 5.1).

Both prints using the spiral method and the zigzag method were tested. For each method, 12 test specimens were printed, weighted and the tensile tests were performed according to the ASTM D638 standard. Tensile specimen dimensions can be seen in figure 5.2.

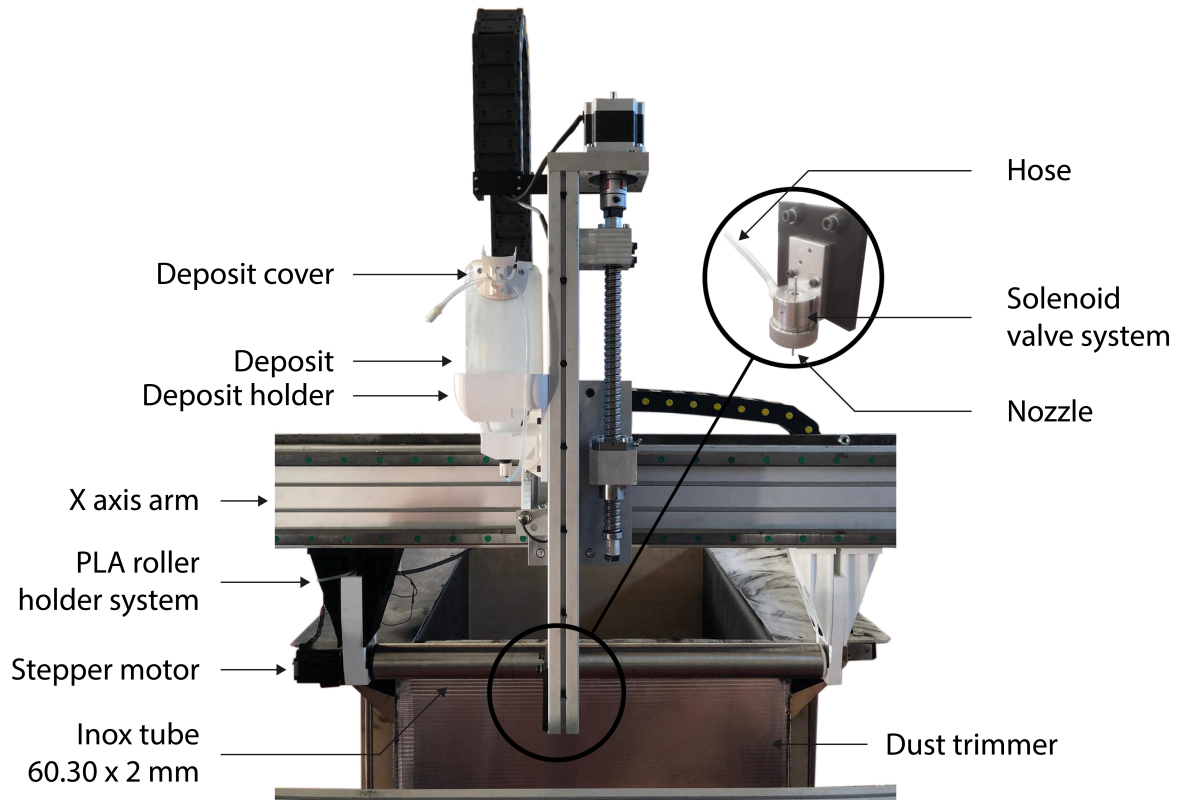


Figure 5.1: Printing machine with the components created for the project.

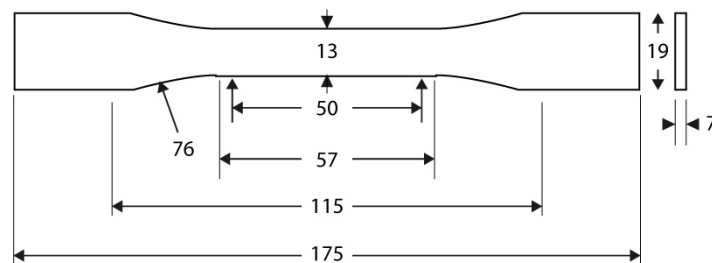


Figure 5.2: Test specimen measures according to the ASTM D638 standard.



Figure 5.3: Test sample bottom.

5.1 Print results

After a batch of test specimens was printed, they were removed individually to a different recipient. In that recipient, all the loose dust still in the printed part was removed with compressed air and cleaned with a brush. Half of the pieces were chosen at random and soaked with cyanoacrylate. Next, they were left at a nail bed to dry.

The provided GTR dust had some agglomerations that had to be separated by hand. However, after spreading the material with the roller, although the layer's surface got flat and regular, underneath it, the material had some lumps. These lumps created some defects in the samples (figure 5.3).

To avoid slowing down the machine's movement and keep the speed at 2 mm/s for binder deposition's sake, a fillet was programmed at every corner of 0.5 mm into the GCode. Despite this, corners had an approximately 10 mm fillet due to the high surface tension between the GTR and PVA 5.4. This surface tension creates a tendency for the already deposited binder to follow the nozzle direction (figure 5.5). The same effect happens as the binder penetrates the matrix material, creating a half-cylinder type shape at the bottom of the printed test specimen as observed in the figure 5.3.

5.2 Cyanoacrylate absorption

After each specimen was removed from the machine and cleaned, they were weighed. Then, the ones that were soaked with cyanoacrylate were weighed again to study how much cyanoacrylate they had absorbed. Green and finished parts weighed a medium of 9.75 grams and 13.29 grams, respectively. From the test specimen 3D CAD model, it is possible to conclude that each specimen should have approximately 19408 mm^3 . Concluding that each printed part absorbs 0.18 g/mm^3 .

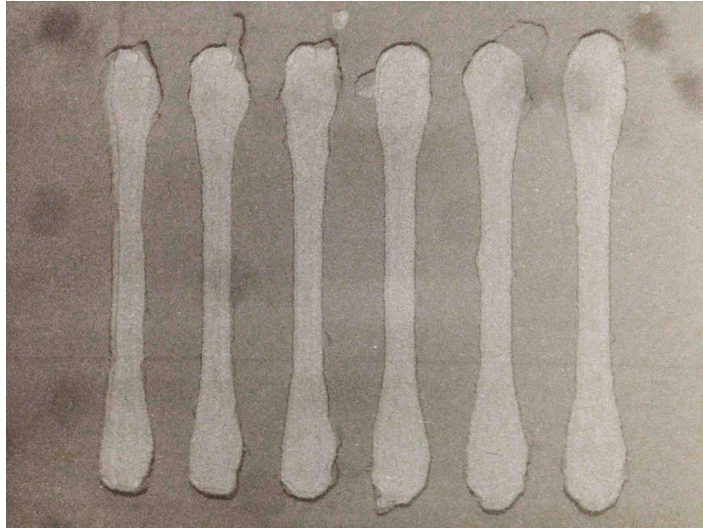


Figure 5.4: Spiral tests printing overview.

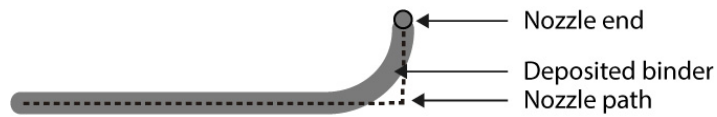


Figure 5.5: Binder path (gray line) versus nozzle path (dashed line).

5.3 Tensile tests

The tensile tests were performed according to the ASTM D 638 standard. The tensile tests were performed with a test load capacity of 5 kN at room temperature. The tests were performed in displacement control, with the loading speed of 5 mm/min in all tests, recording the strength, displacement and extension of the test pieces using an extensometer.

The gage section's initial cross-section area (A_0) was measured before the test to calculate the nominal stress (σ) after having the tensile force (F). The nominal stress (σ) is defined as

$$\sigma = F/A_0 \quad (5.1)$$

Another significant value is Young's modulus (E):

$$E = \sigma/e \quad (5.2)$$

where e is the nominal strain defined as

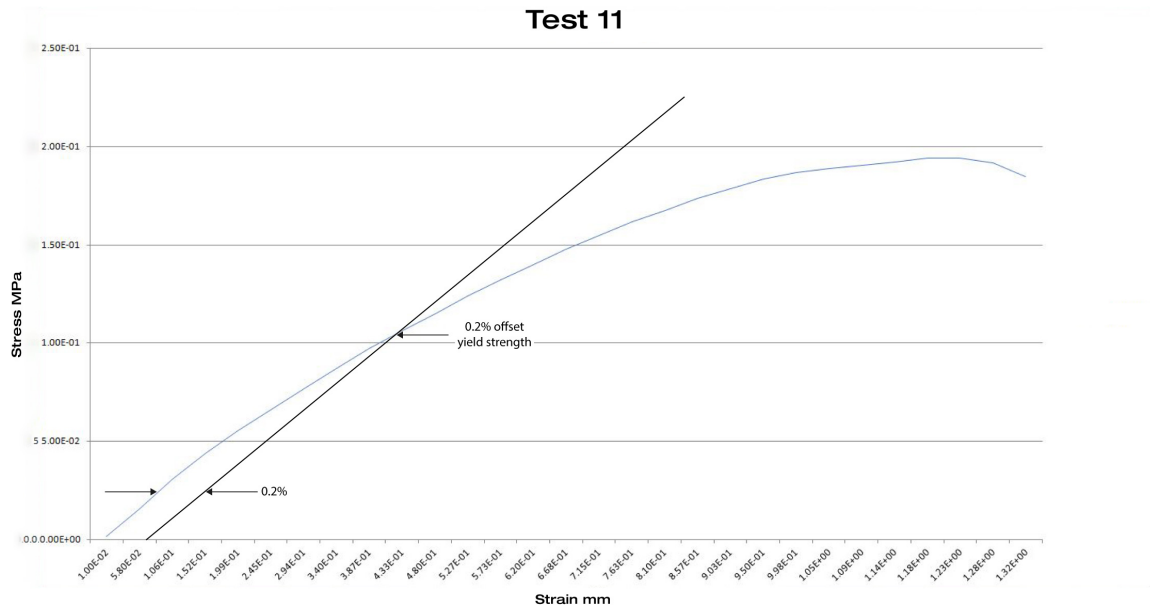


Figure 5.6: Test 11 stress-strain curve.

$$e = \Delta L / L_0 \quad (5.3)$$

where L is the final length, L_0 is the initial length and ΔL is the change in gage length ($L-L_0$).

The yield strength of each material was found by drawing an offset by 0.2% straight line parallel to the initial linear portion of the stress-strain curve (figure 5.6).

5.3.1 Spiral method

The spiral method was separated from the zigzag method because it had a manual intervention to fill up gaps with liquid PVA during printing. Also, only six specimens were tested due to a print error that created a tear through half of the specimens, as observed in figure 5.7.

When the machine was switching from the second to the third layer, a binder bubble was formed at the nozzle's tip. This bubble happened after the material was shoved, creating a line on the layer's surface while retreating into printing position. The tear at figure 5.7 happened at the same location where this bubble passed through.

As mentioned above, this method does not fulfill the requirements needed. These requirements are for the printing system not to have manual intervention. Instead of printing a new 12 test specimen patch using the same technique, a new approach was used to print patches later.

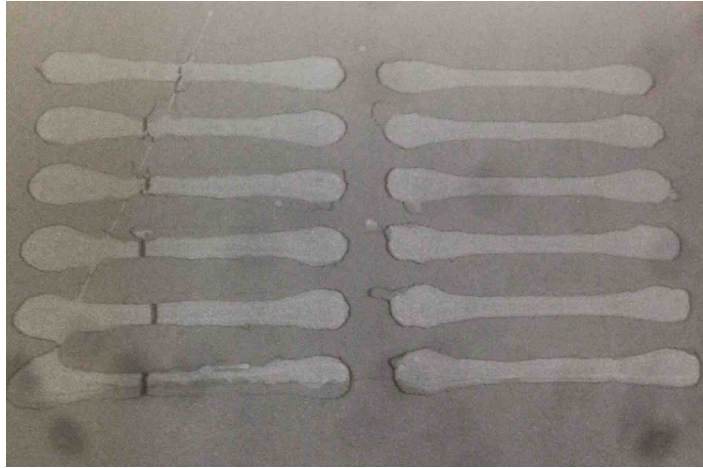


Figure 5.7: Spiral method printed batch.

Specimen test	Area(mm²)	σ_y(MPa)	UTS (MPa)	e	E (MPa)
Test 4	77.09	1.92	2.36	1.45E-01	1.63E+01
Test 5	68.19	1.13	1.54	5.07E-02	3.04E+01
PSD	-	0.37	0.3	0.68	0.43

Table 5.1: Specimens tests performed using the spiral method and soaked with cyanoacrylate. This tests refer to the yield strength (σ_y) in megapascal (MPa), the Ultimate tensile strength (UTS) in megapascal (MPa), the nominal strain (e) and Young's modulus (E) in megapascal (MPa).

Green part

It was not possible to obtain reliable conclusions with the tensile tests of a green part. The first and third tests broke in the machine claw instead of separating inside the gage length. The second test broke where the bottom guide was positioned, presumably due to some fragility the guide created while being attached to the test specimen. For these reasons, all three tests were disregarded.

After cyanoacrylate finish

These tests demonstrated that it is possible to produce a considerable high strength using this technology. Although only three tests were made and the third broke before the test began, the two specimens tested demonstrated high strength values as shown in table 5.1.

Statistical analysis was not made due to the shortage of valid tests and the discrepancy between the values.

Specimen test	Area (mm ²)	σ_y (MPa)	UTS (MPa)	e	E (MPa)
Test 12	84.91	1.06E-01	1.94E-01	2.46E-02	7.89
Test 13	87.44	7.46E-02	1.39E-01	1.99E-02	6.99
Test 14	104.07	6.80E-02	1.72E-01	3.95E-02	4.35
Test 15	98.77	1.78E-01	6.25E-01	5.07E-02	1.56E+01
PSD	-	0.47	0.81	0.33	0.55
PSD with out test 15	-	0.25	0.16	0.36	0.29

Table 5.2: Specimens tests performed using the zigzag method and soaked with cyanoacrylate. This tests refer to the yield strength (σ_y) in megapascal (MPa), the Ultimate tensile strength (UTS) in megapascal (MPa), the nominal strain (e) and Young's modulus (E) in megapascal(MPa)

5.3.2 Zigzag method

Using the zigzag method, it was possible to produce a batch of 12 specimens without manual intervention. The layers above spread the binder more expansively than the first layer, so the print definitions were altered during batch printing. This error was only noticed after printing the second layer of two specimens, so these two specimens were excluded from future tests.

Green part

The same thing that happened with the spiral method green parts happened with the zigzag green parts. It was not possible to obtain reliable conclusions. None of the tests broke inside the gage length. For these reasons, all five tests were disregarded.

After cyanoacrylate finish

At first, out of the five tests considered, only the last was disregarded due to damages before testing. The four tests had results below expectations and the PSD was high (47.3 %) in ultimate tensile strength and higher (81.2 %) in yield strength. However, removing the test 15 that had results much different from the first three samples could obtain reliable results as consulted in table 5.2. Without the fourth test, the PSD of the remaining test's yield stress becomes 16.4 % and the ultimate tensile PSD converts to 24.7 %. These values are considered the first stable results this study produced.

5.4 Discussion

In the process of a green part becoming a finished object, it needs to be handled. So it is essential to define the mechanical properties of green parts and study their feasibility before printing a large object. These results failed to give concrete information on green parts'

mechanical properties. On the other hand, it shows that this method allows the possibility to print small objects and manipulate them into creating new finishing studies.

The finishing method studied the GTR bound with PVA and soaked with cyanoacrylate that highly increased the material strength and stiffness to perform three successful tests.

Knowing the binder was deposited at a constant flow of 0.11 ml/s and each test specimen took 45 seconds to print, it is possible to predict that each specimen has 5 ml of PVA binder in it. Assuming the PVA density is 1.19 g/cm^3 , it is possible to assume that 5.95 grams of each specimen is PVA. Each specimen weighs on average 13.29 grams, making the PVA 44.78 % of the specimen's mass.

The specimens selected for the cyanoacrylate finishing method were weighed before and after the dipping process. This study concluded that each specimen absorbed an average of 3.54 grams, 26.65 % of the specimen's total weight.

The resulting material is a particulate composite with approximately 44.78 % PVA, 26.65 % cyanoacrylate and 28.57 % GTR. The hybrid solution was chosen because the combination of materials facilitated the AM process for BJ.

According to Edwards (1990) [19], a tire's tensile strength should vary between 16.5 to 21.2 MPa; another study concludes that a tire has a Young modulus around 0.001 GPa [20]. It was also found that PVA should have a tensile strength around 15.86 MPa [21] and Young modulus of (0.17 - 20 GPa) [22]. Cyanoacrylate should have a tensile strength of (2.48 - 55.2 MPa) and a Young modulus of 0.0111 - 2.76 GPa [23]. The mixture obtained a tensile strength of 0.17 MPa, significantly below expected. However, a Young modulus of 0.00641 GPa, a predicted value between the Elastic modulus upper bound 0.57211 GPa and the lower bound 0.0014GPa.

5.4.1 Prediction Model

The predictions made for GTR composites' strength were found to be very hypothetical and have a significant difference with the experimental results. According to these models, Young's modulus can be predicted using the following equations.

Elastic Modulus upper bound:

$$E_u = fE_r + (1 - f)E_m \quad (5.4)$$

Elastic Modulus lower bound:

$$E_L = \frac{E_m E_r}{f E_m + (1 - f) E_r} \quad (5.5)$$

E_m, E_r | Elastic modulus of matrix and reinforcement
 f | volume fraction of reinforcement

For the resolution of this formula, it will be used as the cyanoacrylate Elastic modulus, the value of 2 GPa. And Yield strength can be predicted using the following equations.

Strength upper bound:

$$(\sigma f)_u = f(\sigma f)_r + (1 - f)(\sigma f)_m \quad (5.6)$$

Strength lower bound:

$$(\sigma f)_L = (\sigma f)_m \left(1 + \frac{1}{16} \left(\frac{f^{1/2}}{1 - f^{1/2}} \right) \right) \quad (5.7)$$

σ_{fm}, σ_{fr} | Yield strength of matrix and reinforcement
 f | volume fraction of reinforcement

The calculations of these formulas were considered a 2 GPa value for the Young Modulus of cyanoacrylate and 25 MPa for its tensile strength. Also, for the GTR tensile strength, it was considered the value of 20 MPa.

6 Conclusions

This project developed an AM machine to construct large-scale parts using reusable materials as filler material. To develop the BJ system it was used a CNC machine provided by CDRSP as the project base. To adapt this CNC machine to a BJ process, it was necessary to create two central systems to control the matrix material and another to control the binder material.

The first creation to control the matrix material was the creation of a counter-rotating roller using a stepper motor, a stainless steel tube 60.30 x 2 mm and 800 mm long, two bearings (one at each end of the tube) and two sets of Polylactic acid (PLA) 3D printed parts that secure the system to the machine and allow height adjustments. The second created component was created thinking about the reuse of the excess material. A dust trimmer was created to catch the leftover dust, avoid waste, and avoid contaminating the machine's area.

Several binders were searched and tested in two materials; wood and GTR. Moreover, two different binder deposition types were studied, concluding that the binder that best fits the necessity is PVA. Also, to have a reliable deposition method, the binder should be spread by gravity force. PVA is a biodegradable material that can be easily disintegrated in water, ensuring the green part reusing. Also, a finished part with cyanoacrylate has the strength and durability required to create urban furniture.

To test the printing system, it was used GTR grinded into 200 um and two different systems were tested to print 24 test specimens. The specimens were then tested at a universal testing machine to find its tensile properties. The tensile tests concluded that the cyanoacrylate bath is a suitable finishing method to give the finished printed parts strength.

Because this technology aims to use a wide variety of matrix material, it is exposed to form agglomerations and increased surface tension. An optimum powder property should be further explored and achieved by adding additives like Stearic acid or derived stearates to the matrix material before adding it to the printing system. Additionally, an extra step can be studied to improve the process. This step is to purge the binder after each printed layer, avoiding clogging problems and making the process more reliable. Also, additions can be made in the binder to help reduce nozzle clogging and alter surface tension. For future project development, the dust trimmer deposit should be directly connected to the feed deposit, so the powder excess from each layer could be recycled back to the system. As mentioned in chapter 3.4.2, the green part takes 24 hours to dry at room temperature. This process

can be accelerated by adding temperature, in this case, 50°C. Future reference should be studied the possibility of adding temperature to the system to create faster batches. Two methods were tested as CNC parameters. Neither of these methods was perfect. After material improvement, it should also be considered a printing method optimization.

Bibliography

- [1] *ExOne | S-Max Pro*. URL: <https://www.exone.com/en-US/3D-printing-systems/sand-3d-printers/S-MAX-Pro>.
- [2] *3D-printed-wall*. URL: <http://www.the9billion.com/2018/04/18/building-3d-printed-houses-in-under-24-hours-for-us4000/3d-printed-wall/>.
- [3] *Viliaprint Homes Project | XtreeE*. URL: <https://www.xtreee.eu/2018/06/04/viliaprint-homes-project/>.
- [4] *Binder Jetting | Additive Manufacturing Research Group | Loughborough University*. URL: <https://www.lboro.ac.uk/research/amrg/about/the7categoriesofadditivemanufacturing/binderjetting/>.
- [5] *ProJet CJP 360 | 3D Systems*. URL: <https://br.3dsystems.com/3d-printers/projet-cjp-360>.
- [6] A. Le Duigou et al. “3D printing of wood fibre biocomposites: From mechanical to actuation functionality”. In: *Materials and Design* 96 (Apr. 2016), pp. 106–114. ISSN: 18734197. DOI: 10.1016/j.matdes.2016.02.018.
- [7] Faez Alkadi et al. “3D Printing of Ground Tire Rubber Composites”. In: *International Journal of Precision Engineering and Manufacturing - Green Technology* 6.2 (Apr. 2019), pp. 211–222. ISSN: 21980810. DOI: 10.1007/s40684-019-00023-6.
- [8] Arthur Wilson Fonseca Coelho, Rossana Mara da Silva Moreira Thiré, and Anna Carla Araujo. “Manufacturing of gypsum–sisal fiber composites using binder jetting”. In: *Additive Manufacturing* 29 (Oct. 2019), p. 100789. ISSN: 22148604. DOI: 10.1016/j.addma.2019.100789.
- [9] Henning Zeidler et al. “3D printing of biodegradable parts using renewable biobased materials”. In: *Procedia Manufacturing* 21 (2018), pp. 117–124. ISSN: 23519789. DOI: 10.1016/j.promfg.2018.02.101. URL: <https://doi.org/10.1016/j.promfg.2018.02.101>.
- [10] *Regenerated Waste Tire Powders as Fillers for Wood Fiber Composites.: EBSCOhost*. URL: <https://web.b.ebscohost.com/ehost/pdfviewer/pdfviewer?vid=0&sid=71cc6f7b-07b6-44da-bdbb-d4a9a02cda05%40pdc-v-sessmgr05>.
- [11] Ben Utela et al. *A review of process development steps for new material systems in three dimensional printing (3DP)*. 2008. DOI: 10.1016/j.jmapro.2009.03.002.
- [12] *US6596224B1 - Jetting layers of powder and the formation of fine powder beds thereby - Google Patents*. URL: <https://patents.google.com/patent/US6596224B1/en>.

- [13] *US6955776B1 - Method for making a dental element - Google Patents*. URL: <https://patents.google.com/patent/US6955776B1/en>.
- [14] *US7550518B2 - Methods and compositions for three-dimensional printing of solid objects - Google Patents*. URL: <https://patents.google.com/patent/US7550518B2/en>.
- [15] *US5252264A - Apparatus and method for producing parts with multi-directional powder delivery - Google Patents*. URL: <https://patents.google.com/patent/US5252264A/en>.
- [16] *US20170368780A1 - Variable density, variable composition or complex geometry components for high pressure presses made by additive manufacturing methods - Google Patents*. URL: <https://patents.google.com/patent/US20170368780A1/en>.
- [17] S. Yang and J. R.G. Evans. *Metering and dispensing of powder; the quest for new solid freeforming techniques*. Sept. 2007. DOI: 10.1016/j.powtec.2007.04.004.
- [18] *US5660621A - Binder composition for use in three dimensional printing - Google Patents*. URL: <https://patents.google.com/patent/US5660621A/en>.
- [19] D. C. Edwards. *Polymer-filler interactions in rubber reinforcement*. Oct. 1990. DOI: 10.1007/BF00581070. URL: <https://link.springer.com/article/10.1007/BF00581070>.
- [20] Tommy Edeskär. *Technical and Environmental Properties of Tyre Shreds Focusing on Ground Engineering Applications*. Tech. rep. 2004.
- [21] MOCHAMAD ASROFI et al. "Tensile, Thermal and Moisture Absorption Properties of Polyvinyl Alcohol (PVA) / Bengkuang (*Pachyrhizus erosus*) Starch Blend Films". In: *Material Science Research India* 16.1 (Apr. 2019), pp. 70–75. ISSN: 09733469. DOI: 10.13005/msri/160110.
- [22] Kazuo Yamaura et al. "Preparation and properties of very thin films of syndiotacticity-rich poly(vinyl alcohol)". In: *Journal of Applied Polymer Science* 34.3 (1987), pp. 989–998. ISSN: 10974628. DOI: 10.1002/app.1987.070340310.
- [23] *Overview of materials for Cyanoacrylate Adhesive*. URL: <http://www.matweb.com/search/datasheet.aspx?matguid=d0d7dbec7666421caf8aa08724b634c5&ckck=1>.